CALIFORNIA INSTITUTE OF TECHNOLOGY

EARTHQUAKE ENGINEERING RESEARCH LABORATORY

STRUCTURAL IDENTIFICATION OF JPL BUILDING 180 USING OPTIMALLY SYNCHRONIZED EARTHQUAKE RECORDS

By

G.H. McVerry and J.L. Beck

Report No. EERL 83-01

Pasadena, California

August 1983

CALIFORNIA INSTITUTE OF TECHNOLOGY

EARTHQUAKE ENGINEERING RESEARCH LABORATORY

STRUCTURAL IDENTIFICATION OF JPL BUILDING 180
USING OPTIMALLY SYNCHRONIZED EARTHQUAKE RECORDS
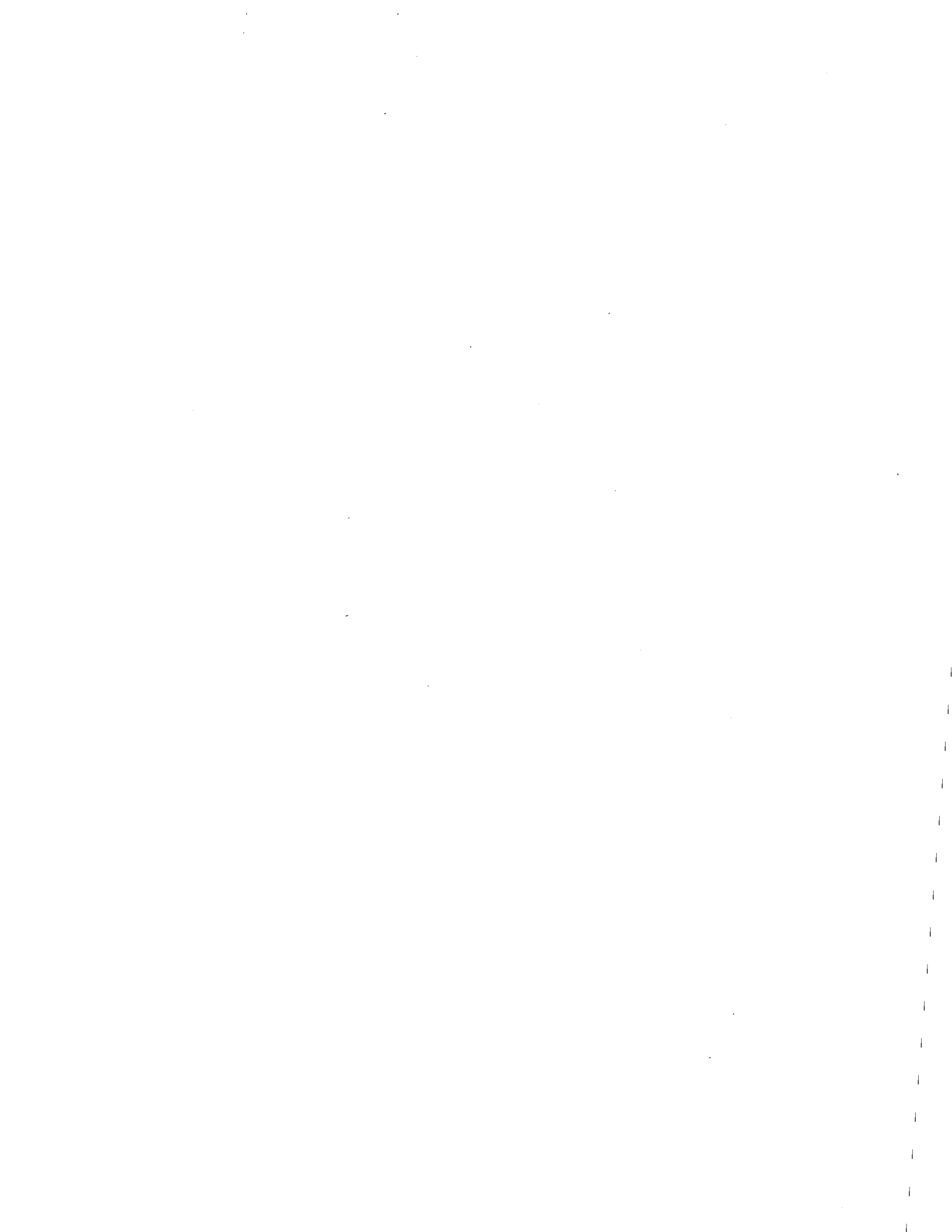
by

G.H. McVerry and J.L. Beck

Report No. EERL 83-01

Pasadena, California

August 1983

TABLE OF CONTENTS

ACKNOWLEDGEMENTS

ABSTRACT

Linear models of JPL Building 180 were identified from its strong-motion records obtained in the 1971 San Fernando earthquake using two system identification techniques, both of which revealed a previously undetected time-shift of about 0.08 second between the digitized basement and roof records. Optimal alignment of the records produced improved matches between the measured and model responses, and overcame difficulties encountered in extracting physically reasonable estimates for the parameters of the third and higher modes from the original records.

The two complementary identification techniques provide optimal estimates with standard errors for the periods, dampings and effective participation factors of the dominant modes in the response. One method performs a least-squares match between the calculated and recorded response in the time domain, and the other in the frequency domain. Akaike's information criterion is used to determine the number of modes to include in the models.

The fundamental periods identified for JPL Building 180 lengthened during the response by 40% and 60% for the longitudinal and transverse directions respectively, starting from values close to those measured in vibration tests. The effective overall damping factors for the fundamental modes in the two directions were 3.6% and 4.4% of critical.

1. <u>INTRODUCTION</u>

Two structural identification techniques were used to determine optimal linear models of the 9-story, steel-framed JPL Building 180 from its strong-motion accelerograph records obtained in the 1971 San Fernando earthquake. The study revealed a previously undetected lack of synchronization, amounting to several timesteps of 0.02 seconds, between the digitized basement and roof records, even though the accelerographs were interconnected to provide a common time-base. Optimal synchronization of the records led to improved matches between the measured and model responses, and overcame difficulties encountered in extracting physically reasonable estimates for the parameters of the third and higher modes from the original records. A possible explanation for the non-synchronization of the records from the interconnected instruments is provided.

A summary of the application of system identification to strong motion earthquake acceleration records from structures is provided in a recent review article [3].

The two identification techniques used in this study are output-error methods, one minimizing a measure-of-fit in the time domain [2,4] and the other in the frequency domain [12,13]. Recorded seismic base motion and response are used to estimate the periods, dampings and effective participation factors of the dominant modes by systematic iteration to the values which produce least-squares matches of the time histories or the Fourier transforms of the calculated and recorded responses. There are theoretical reasons for expecting the results from the time- and frequency-domain methods to be nearly equivalent. This is

confirmed in this study by the good agreement between the parameter estimates when the two methods are applied to the same data.

Sensitivity analyses provide standard errors for the parameter estimates, together with a measure of the amount of interaction between the estimates of the various parameters. Akaike's information criterion (AIC) [1] is applied to determine a trade-off between the closeness of the fit and the number of modes used in the model. Including more modes than indicated by the AIC produces a marginal improvement in the measure-of-fit, but the estimates of the additional parameters are likely to be unreliable.

During the San Fernando earthquake, the acceleration at the roof of JPL Building 180 reached 0.37g and 0.21g in the longitudinal (S82E) and transverse (S08W) directions respectively. These values were among the largest recorded in instrumented buildings during the earthquake, but damage was limited to minor non-structural cracking.

In the present study, it was found possible to determine time-invariant linear models appropriate for the overall response, and also to trace the temporal variation of the effective linear parameters due to nonlinear structural behavior by determining optimal linear models for a series of short segments of the response. The fundamental periods lengthened during the response by forty and sixty percent for the longitudinal and transverse directions respectively, starting from values close to those measured in vibration tests. The second mode periods lengthened by around thirty percent. The effective overall dampings were 3.6 and 4.4 percent for the fundamental modes in the

longitudinal and transverse directions, with values of about 5 and 7
percent during the maximum response.

2. JPL BUILDING 180

2.1 Description of the Building

JPL Building 180 (Figure 1), designed in 1961, is a 9-story, steel-
frame structure on the campus of the Jet Propulsion Laboratory,
Pasadena, California. The building is 146 feet high from the foundation
to the roof, with horizontal dimensions of 220 feet by 40 feet. The
lateral resistance in the transverse north-south direction is provided
by welded steel spandrel trusses and by steel columns partially encased
in concrete. The longitudinal loads are carried by a frame consisting
of steel girders and columns. The long north and south faces of the
building are formed by glass curtain walls, while the east and west end-
walls consist of precast concrete panels supported by the steel frame.
The foundation is formed by continuous strip footings running longitudi-
nally. More detailed descriptions of the building and site conditions
are contained in the design report by Brandow and Johnston [6], and in
the studies by Nielsen [16] and Wood [19,20]. A summary of the building
properties and a presentation of the records obtained in the basement
and on the roof during the San Fernando earthquake can be found in a
report by Foutch, Housner and Jennings [9].

A series of vibration tests, starting with those of Nielsen [16]
during the construction phase, have revealed considerable variations in
the dynamic properties of the building as a result of earthquake shaking
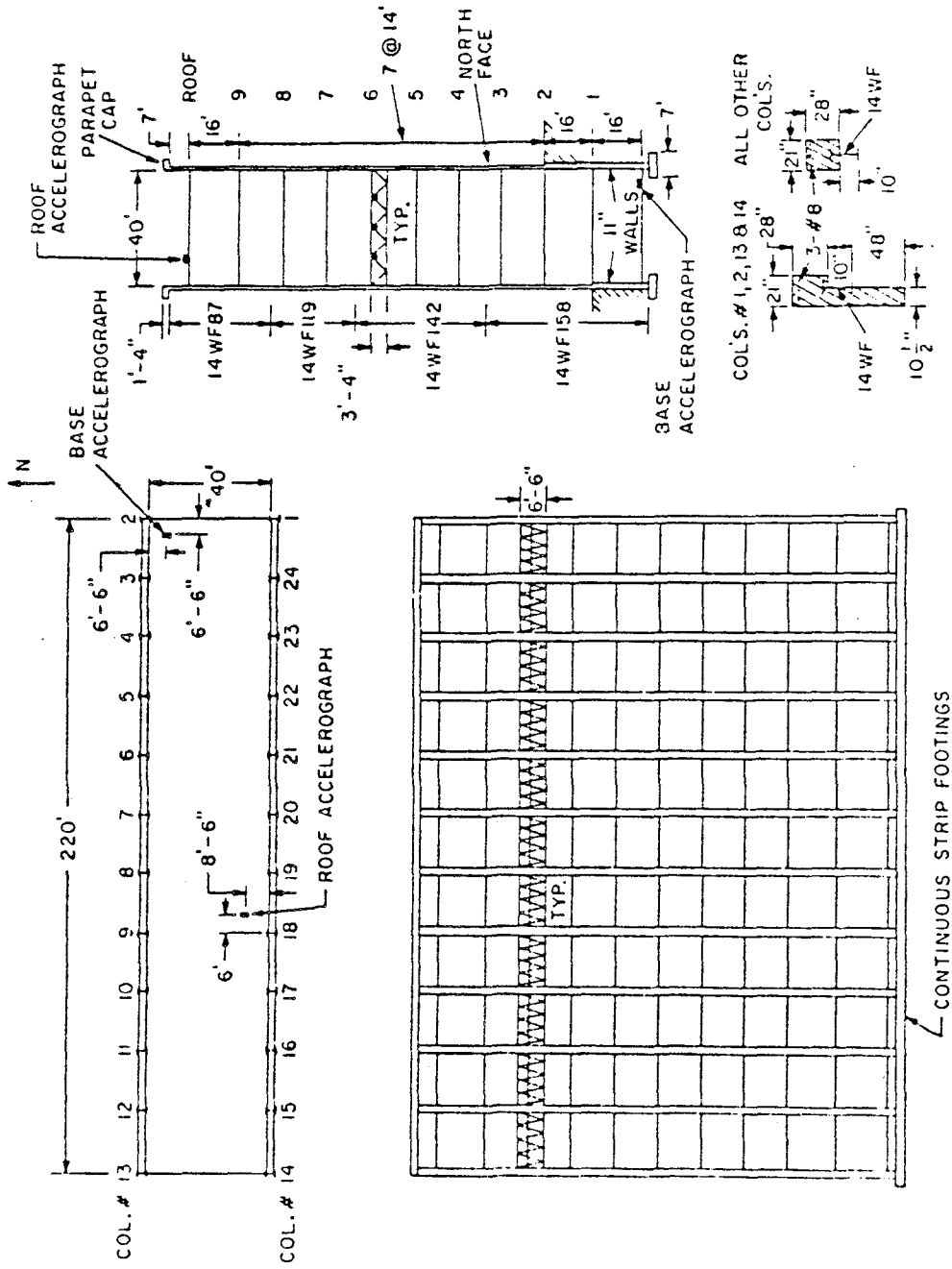
Fig. 1.   Typical floor plan and longitudinal and transverse sections of JPL Building 180 (from [9]).

and structural alterations. The variation of the fundamental periods in these tests has been summarized by Foutch and Housner [8].

As well as the strong shaking from the San Fernando (February 9, 1971) earthquake which was centered fifteen miles to the northwest of JPL, less severe response had been recorded in the building during the earlier Borrego Mountain (April 8, 1968) and Lytle Creek (September 12, 1970) earthquakes.

2.2 Previous Analyses of the Earthquake Records

Previous analyses of the earthquake behavior of the building have been performed by Udwadia and Trifunac [18], Wood [19,20], Brandow and Johnston [6], Beck [2] and McVerry [12].

Udwadia and Trifunac [18] used a moving-window Fourier analysis approach, picking out the effective periods of the first two modes in each direction as a function of time from peaks of the ratio of Fourier transforms of 8-second segments of the basement and roof records. Their method was essentially a non-parametric frequency-domain approach in which a "transfer function" was first estimated, with a parametric model then imposed to interpret the locations of the major peaks as modal frequencies. The elongation of the principal periods during the earthquake were identified by this approach, but their study demonstrated several short-comings typical of direct transfer function applications to records of structural response in earthquakes. The short-comings of the moving-window transfer function approach generally limit the estimation to the modal periods, since the dampings and participation factors are difficult to estimate reliably.

Transfer functions estimated from earthquake records are usually very jagged, unlike their theoretical counterparts which are smooth curves with well-defined peaks at the lower modal frequencies. The jaggedness is caused by the combined effects of the time-variation and amplitude nonlinearity of the system, finite length and discrete sampling of the records, the neglect of the effects of the initial and final conditions introduced by the truncation of the records, and measurement noise in the data. Because of the irregularity of the transfer function estimated from the data, it is often difficult to identify more than the first one or two modal frequencies with confidence. In addition, the half-power bandwidths are generally poorly defined because of the jaggedness of the estimated transfer function curves which, together with the possibility of interference between closely-spaced modes, makes estimation of damping and participation factors difficult. Usually smoothing is introduced in the calculation of the transforms of the excitation and response, and again in the estimated transfer function. While this leads to smoother functions to inspect, smoothing introduces bias into the damping and participation factor estimates since it reduces the amplitude and increases the bandwidth of all peaks. By imposing the parametric model at the outset of the analysis and matching the response over a broad frequency band, as in the present study, rather than introducing the parametric interpretation only at the final stage and then estimating the parameter values from only a few data points on poorly-defined peaks, a frequency-domain approach can be successful.

It is to be noted that the effects of truncation of the records may assume major importance if segments of the response are used, such as in moving-window analyses, particularly for later portions of the records which often consist mainly of free-vibration decay of motion induced by earlier excitation. The terms arising from the initial and final conditions in the frequency-domain input-output relation (i.e. the second and third terms in equation 6 in Section 3.1) may then contribute more to the response than the conventional transfer function expression contained in the first term of equation 6, preventing estimation of the damping and participation factors unless the parameters v_{pr} and d_{pr} are also determined. Fortunately for Trifunac and Udwadia's application, where they traced the variation in only the modal periods, the truncation effect is not serious. The ignored terms contain the same denominators as the conventional transfer function expression so they also peak at the modal frequencies. The present studies show that in fact all the modal parameters can be estimated from segments of the records using either time-domain or frequency-domain approaches, provided that the end conditions are taken into account.

The comments about the jaggedness of estimated transfer functions certainly apply to the JPL Building 180 records. Figure 2 shows the transfer function calculated from the first 40.96 seconds of the San Fernando S82E records. The frequencies of the modes dominant in the response are approximately 0.8, 2.5 and 4.0 Hz (Figure 3), but there are many more sharp spikes which make interpretation of the estimated transfer function difficult.
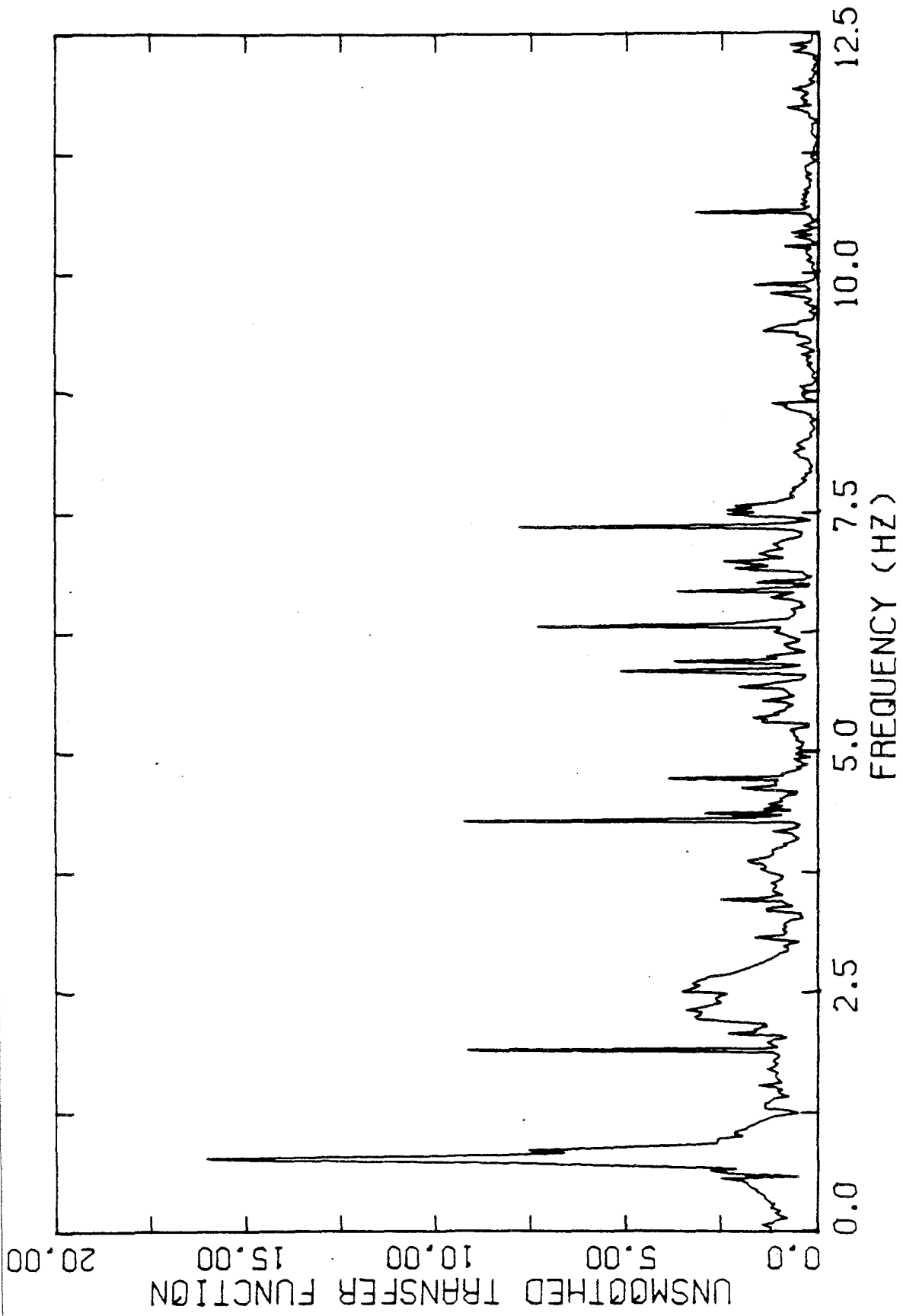
Fig. 2. JPL Building 180, San Fernando S82E component. Amplitude of the unsmoothed transfer function between the absolute acceleration recorded in the basement and on the roof.
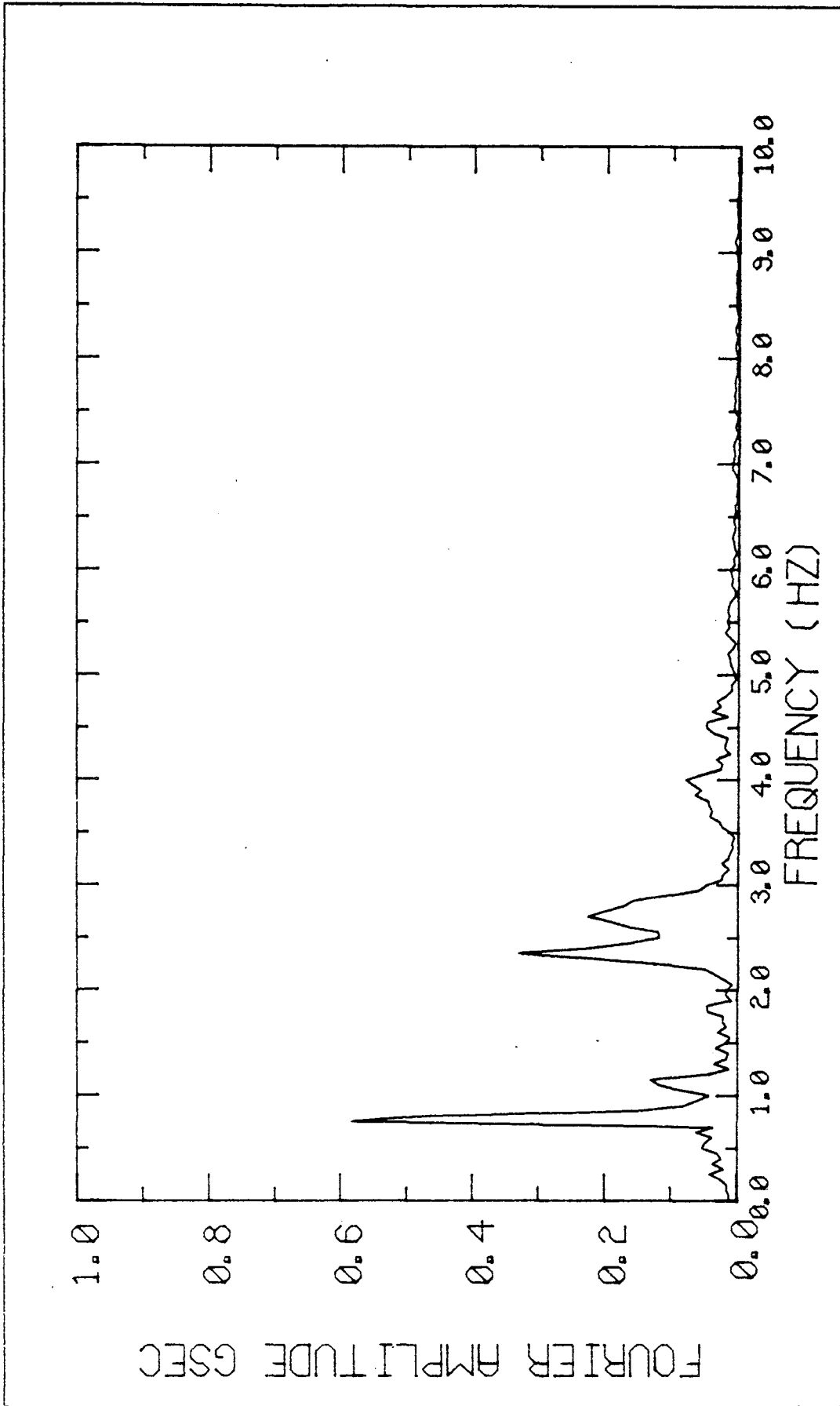
Fig. 3. JPL Building 180, San Fernando S82E component. Fourier amplitude spectrum of the first 20 seconds of the measured acceleration response.

Wood [19] used trial-and-error modification of simple models of the structure synthesized from the design data to achieve better visual matching between the recorded responses and those calculated for the models. Two models were synthesized for each direction based on the stiffnesses of the frame members and the story masses calculated from the design drawings. The "full-composite" models were considered appropriate for small amplitude motions, such as in vibration tests and small earthquakes, in which the concrete encasing the steel columns remains uncracked. For larger-amplitude motions, Wood suggested the "partial-composite" models, which were based on the assumption that the concrete in the flexural tension zones of the columns would crack and provide no flexural stiffness. From a study of the calculated response of the models to the basement acceleration recorded in the San Fernando earthquake, using 5 percent damping in all modes, the partial-composite models were indeed found to give better matches of the roof records. The partial-composite models were then refined by trial-and-error adjustment of the values of the first three modal periods and all the damping factors to better match the Fourier amplitudes of the roof accelerations. Although the partial- and full-composite models produced substantially different modal periods, the roof participation factors were insensitive to the different stiffness distributions, so Wood used the participation factors given by the partial-composite model rather than estimating them when matching the measured earthquake response. His study is one of the most successful examples of the trial-and-error approach to the adjustment of synthesized structural models to match recorded earthquake response (Figure 8a). The results suggested that

the peak stresses in the structural frame approached, but did not exceed, the yield level during the San Fernando earthquake.

Brandow and Johnston [6] also used trial-and-error modification of a design model to match the earthquake response. Their study, performed soon after the earthquake, achieved a much poorer match than that obtained by Wood. Their results are more typical of this type of approach, many such studies for other structures being given in a NOAA report [15].

The properties of Wood's and Brandow and Johnston's models are summarized in Table 1.

The availability of much vibration test data, the opportunity to perform identifications for the different response levels of the three earthquakes, and the chance to compare the results with those of the earlier analyses, made the earthquake response of JPL Building 180 attractive for study using the present systematic identification techniques. The building records from all three earthquakes have been studied [12] prior to discovering the lack of synchronization, but only the San Fernando records are studied in this paper.

3. THE IDENTIFICATION TECHNIQUES

3.1 The Structural Models

The class of models considered is rigid-base, planar, linear models possessing classical normal modes, as commonly used in earthquake-resistant design. Beck [2] has shown by considerations of identifiability and accuracy that the appropriate parameters to estimate for linear

TABLE 1

SYNTHESIZED MODELS OF JPL BUILDING 180

(a) Wood's Full Composite Models

Mode	SO8W		S82E	
	Period (sec)	Participation Factor	Period (sec)	Participation Factor
1	1.163	1.322	1.089	1.288
2	0.338	−0.487	0.361	−0.438
3	0.165	0.253	0.213	0.234
4	0.095	−0.140	0.147	−0.127
5	0.061	0.077	0.108	0.065
6	0.044	−0.035	0.084	−0.032

(b) Wood's Partial Composite Models

Mode	SO8W		S82E	
	Period (sec)	Participation Factor	Period (sec)	Participation Factor
1	1.457	1.306	1.209	1.303
2	0.469	−0.460	0.418	−0.463
3	0.259	0.242	0.257	0.240
4	0.168	−0.139	0.184	−0.113
5	0.118	0.079	0.142	0.047
6	0.087	−0.042	0.114	−0.018

(c) Wood's Refined Models (to fit earthquake responses)

Mode	SO8W			S82E		
	Period (sec)	Damping (%)	Partic. Factor	Period (sec)	Damping (%)	Partic. Factor
1	1.440	3.0	1.306	1.290	4.0	1.303
2	0.436	3.0	−0.460	0.420	6.0	−0.463
3	0.235	4.0	0.242	0.260	6.0	0.240
4	0.167	2.0	−0.139	0.184	5.0	−0.113
5	0.117	2.0	0.079	0.142	2.0	0.047
6	0.087	2.0	−0.042	0.114	2.0	−0.018

TABLE I (CONT.)

(d) Brandow and Johnston's Models

Modal Periods	S08W			S82E		
	T_1	T_2	T_3	T_1	T_2	T_3
Initial Model	1.12	0.37	0.22	1.06	0.38	0.23
Adjusted Model	1.25	0.42	0.24	1.23	0.45	0.28
Damping (% Critical) of Modes						
Time Segment		S08W		S82E		
0-5 sec		6.6		5.0		
5-10 sec		4.9		3.7		
10+ sec		3.3		2.5		

models of structures from earthquake records are the periods, dampings, and effective participation factors at the recording locations, of the dominant modes in the measured response. The complete mode shape cannot be identified from the records of the excitation and the response at the limited number of locations usually available. This lack of identifiability of the mode shapes and the presence of model and measurement error prevent reliable estimation of the elements of the damping and stiffness matrices. Consequently, a modal approach was taken in both the time- and frequency-domain methods.

The equations of motion for a linear, planar model governing the displacement relative to the base, $\underline{x}$, in terms of the mass, damping and stiffness matrices (M, C and K) in response to a base acceleration $\ddot{z}$ may be written

$$M\underline{\ddot{x}} + C\underline{\dot{x}} + K\underline{x} = -M\underline{1}\ddot{z} \qquad (1)$$

where every element of the column vector $\underline{1}$ is unity. Modal decomposition gives an uncoupled equation for x_{pr}, the rth mode contribution to the relative displacement at position p:

$$\ddot{x}_{pr} + 2\zeta_r\omega_r\dot{x}_{pr} + \omega_r^2 x_{pr} = -c_{pr}\ddot{z} \qquad (2)$$

For a model with R modes, the total response at p at time t for the displacement relative to the base, $x_p(t)$, is then:

$$x_p(t) = \sum_{r=1}^{R} x_{pr}(t) \qquad (3)$$

The parameters of the rth mode are the modal period, $T_r(=2\pi/\omega_r)$, the fraction of critical viscous damping, ζ_r, and the effective participation factor at position p, c_{pr}, defined as:

$$c_{pr} = \phi_{pr}\left[\underline{\phi}_r^T \, \underline{M}\underline{1}\right] \Big/ \left[\underline{\phi}_r^T \, \underline{M}\underline{\phi}_r\right] \tag{4}$$

Here ϕ_{pr} is the value of the rth mode shape at p and $\underline{\phi}_r$ is the rth mode shape vector. Note that c_{pr} is independent of the normalization of the mode shape, unlike the more conventional definition of the participation factor which does not include the factor ϕ_{pr}. Furthermore, the parameters T_r, ζ_r and c_{pr} for each mode can be shown to be the parameters which are specified uniquely by the base motion and the response at position p of a model of the type given by equation (1) [2].

In the time domain, digitized records of the base acceleration and response acceleration are available at equally-spaced intervals, usually of 0.02 seconds. Velocity and displacement records are calculated by numerical integration. In this study, the model equations (2) were solved using the Nigam-Jennings algorithm [17].

The frequency-domain version of the model response is obtained by taking finite Fourier transforms. The transforms $A_{pT}(\omega)$ of the relative acceleration at p over the segment of duration T from time t_i to t_f is defined as:

$$A_{pT}(\omega) = \int_{t_i}^{t_f} \ddot{x}_p(t)e^{-i\omega t}dt \tag{5}$$

with a similar definition for the transform $Z_T(\omega)$ of the base acceleration $\ddot{z}(t)$. The transforms of the measured records are discrete, obtained using a fast Fourier transform algorithm which produces the complex-valued transform at N equally-spaced frequencies ω_n $(= 2\pi n/T = n\Delta\omega,\ n = 0 \ldots N-1)$ from 2N equally-spaced samples of a record of length $T = t_f - t_i$.

For the sampled frequencies, the input-output relation is:

$$
A_{pT}(\omega) = \sum_{r=1}^{R} \frac{\omega^2(b_r - \omega^2) - i\omega^3 a_r}{(b_r - \omega^2)^2 + \omega^2 a_r^2}\, c_{pr} Z_T(\omega)
$$

$$
+ \sum_{r=1}^{R} \frac{b_r(b_r - \omega^2)^2 + \omega^2 a_r^2 - i\omega^3 a_r}{(b_r - \omega^2)^2 + \omega^2 a_r^2}\, v_{pr}
$$

$$
+ \sum_{r=1}^{R} \frac{a_r b_r \omega^2 + i\omega b_r(b_r - \omega^2)}{(b_r - \omega^2)^2 + \omega^2 a_r^2}\, d_{pr} \tag{6}
$$

where

$$
a_r = 2\zeta_r \omega_r \qquad\qquad b_r = \omega_r^2
$$

$$
d_{pr} = x_{pr}(t_f) - x_{pr}(t_i) \qquad v_{pr} = \dot{x}_{pr}(t_f) - \dot{x}_{pr}(t_i) \tag{7}
$$

3.2 Parameter Estimation

The parameter estimation phase of the structural identification process involves systematically selecting the parameters of the model to best represent the behavior of the structure according to some specified criterion. A natural method, known as a least-squares output-error approach, is to select the parameters of the model to minimize the

square of the difference between the recorded response and that calculated for the model.

Beck [2,4] developed a time-domain version, minimizing the measure-of-fit J_1 with respect to the parameters of R modes $[T_r, \zeta_r, c_{pr}, x_{pr}(t_i), \dot{x}_{pr}(t_i), r=1,\ldots R]$, where

$$J_1 = K_1 V_1 \int_{t_i}^{t_f} (x_o - x_p)^2 dt + K_2 V_2 \int_{t_i}^{t_f} (v_o - \dot{x}_p)^2 dt +$$

$$K_3 V_3 \int_{t_i}^{t_f} (a_o - \ddot{x}_p)^2 dt \qquad (8)$$

and the normalizing factors are defined by:

$$V_1 = 1 / \int_{t_i}^{t_f} x_o^2 dt \; , \; V_2 = 1 / \int_{t_i}^{t_f} v_o^2 dt \; , \; V_3 = 1 / \int_{t_i}^{t_f} a_o^2 dt \qquad (9)$$

Each K_i is 1 or 0, according to the quantities used in the identification. The "observed" quantities x_o, v_o and a_o are the relative displacement, velocity and acceleration histories derived from the acceleration records in the base and at position p in the structure, and $x_p, \dot{x}_p$ and $\ddot{x}_p$ are the corresponding quantities calculated for the model from equations (2) and (3), using as input the measured base acceleration $\ddot{z}$. In practice, only one of the relative displacement, velocity or acceleration has been used at a time (although there is no reason why all three

cannot be used simultaneously), and the corresponding J_1s are referred to as J_d, J_v and J_a.

In the frequency-domain method developed by McVerry [12,13], a least-squares fit of the Fourier transform of the acceleration response is performed over a selected frequency band by minimizing J_2 with respect to the modal parameters ($a_r, b_r, c_{pr}, d_{pr}, v_{pr}, r=1,...R$), where

$$J_2 = \sum_{1=1_{min}}^{1_{max}} |A(1\Delta\omega) - A_{pT}(1\Delta\omega)|^2 \Big/ \sum_{1=1_{min}}^{1_{max}} |A(1\Delta\omega)|^2 \qquad (10)$$

Here $A(1\Delta\omega)$ is the finite Fourier transform of a_o, the "observed" relative acceleration at p (obtained from the recorded quantities by subtracting the base acceleration from the absolute acceleration), while $A_{pT}(1\Delta\omega)$ is the corresponding model response from equation (6). It is also possible to apply the technique using Fourier transforms of the relative velocity or displacement. Note that the match in (10) is of the complex-valued transform, thereby including the phase information as well as the amplitude.

From Parseval's theorem for discrete Fourier transforms, the frequency-domain error criterion of equation (10) is equivalent in the time domain to performing a least-squares match of the response at the sampling times provided all the FFT frequency points are used in J_2. Although the evaluation of the time-domain integral measure-of-fit J_a is performed numerically using repeated applications of Simpson's rule, which deviates from a summation of the discrete data points by weighting odd and even points differently, and the frequency band in J_2 is usually

limited to the significant response to save computation time, it is
shown in this study that the estimated parameter values from the time-
and frequency-domain methods are essentially equal.

Detailed descriptions of the nonlinear optimization algorithms for
performing the minimization of expressions (8) and (10) have been
presented previously [2,12], and will not be repeated here. With both
methods, it is possible either to determine a single time-invariant
linear model appropriate for the entire response or, by considering a
series of models for short segments of the records, to study the changes
of the effective linear parameters due to nonlinear and time-varying
behavior.

3.3   Standard Errors for the Parameter Estimates

The methods outlined in the last section produce optimal estimates
of the parameters according to two essentially equivalent criteria of a
widely used least-squares output-error form. In this section the esti-
mation process is placed within a probabilistic framework, leading to
expressions for the precision of the estimates as well as their optimal
values.

By making the assumption that the errors between the measured
output and calculated model output are Gaussian, the optimal estimates
in the least-squares sense are easily shown to be the maximum likelihood
estimates also. This result allows the well-known properties of maximum
likelihood estimates to be used to provide asymptotic distributions for
the least-squares estimates derived from a large number of data.
Unfortunately, the interpretation of these results, derived from

classical statistics, introduces some conceptual difficulties which can, however, be avoided by adopting a Bayesian approach. With a posterior distribution for the parameter estimates based on the data and on a noninformative prior distribution, the most probable estimates _a posteriori_ are shown to be identical to the maximum likelihood, and hence least-squares, estimates. Results very similar to those of the classical approach are obtained for the distribution of the estimates, but with subtle changes so that their interpretation poses none of the previous conceptual difficulties.

As the starting point, the measured response (which may be the acceleration, velocity or displacement) at time t_n is represented as x_n, the model response at time t_n for a parameter vector $\underline{\theta}$ as $m(t_n|\underline{\theta})$, and their difference as ε_n:

$$x_n = m(t_n|\underline{\theta}) + \varepsilon_n \tag{11}$$

The errors ε_n are assumed to be from a Gaussian white noise process which has variance σ^2 and mean zero, and so are independent for different times. Under these assumptions, the probability distribution for a response vector $\underline{x} = (x_1, x_2, \ldots x_n)^T$, given a model parameter vector $\underline{\theta}$ is:

$$p(\underline{x}|\underline{\theta}) = \prod_{n=1}^{N} p(x_n|\underline{\theta})$$

$$= \prod_{n=1}^{N} p(\varepsilon_n|\underline{\theta})$$

$$= \frac{1}{(2\pi\sigma^2)^{N/2}} \exp\left\{-\frac{1}{2\sigma^2} \sum_{n=1}^{N} \left[x_n - m(t_n|\underline{\theta})\right]^2\right\}$$

$$= \frac{1}{(2\pi\sigma^2)^{N/2}} \exp\left\{-\frac{1}{2\sigma^2} J(\underline{\theta})\right\} \tag{12}$$

It can be seen that the output-error measure,

$$J(\underline{\theta}) = \sum_{n=1}^{N} \left[x_n - m(t_n|\underline{\theta})\right]^2 \tag{13}$$

arises naturally in this probabilistic formulation based on a Gaussian white noise assumption about the errors.

The classical maximum likelihood estimation of the parameters $\underline{\theta}$ involves maximizing the distribution $p(\underline{x}|\underline{\theta})$, or equivalently its logarithm $L(\underline{\theta}, \sigma^2)$

$$L(\underline{\theta}, \sigma^2) = -\frac{N}{2} \log(2\pi\sigma^2) - \frac{1}{2\sigma^2} J(\underline{\theta}) \tag{14}$$

From this expression, it is easily seen that the maximum likelihood estimates are given by $\hat{\sigma}^2 = \frac{1}{N} J(\hat{\underline{\theta}})$ for the output-error variance, and by the parameters $\hat{\underline{\theta}}$ which minimize $J(\underline{\theta})$, which is the least-squares output-error criterion.

The equivalence of the least-squares and maximum likelihood methods allows use of the well-known result for maximum likelihood estimates (e.g., Goodwin and Payne [10], section 3.5) that for a large number N of data points the distribution of $\hat{\underline{\theta}}$ asymptotically approaches a multi-dimensional Normal distribution with mean $\underline{\theta}_o$ and covariance matrix $S^{-1}(\underline{\theta}_o, \sigma_o)$. The parameters $\underline{\theta}_o$ and σ_o are the "true" values of $\underline{\theta}$ and σ and the sensitivity matrix S is defined by

$$[S(\underline{\theta},\sigma)]_{ij} = E\left[-\frac{\partial^2 \log p(\underline{x}|\underline{\theta},\sigma)}{\partial\theta_i \partial\theta_j}\right]$$

$$= \frac{1}{2\sigma^2} E\left[\frac{\partial^2 J(\underline{\theta})}{\partial\theta_i \partial\theta_j}\right]$$

$$= \frac{1}{\sigma^2} \sum_{n=1}^{N} \frac{\partial m(t_n|\underline{\theta})}{\partial\theta_i} \frac{\partial m(t_n|\underline{\theta})}{\partial\theta_j} \tag{15}$$

There are both practical and conceptual problems with this result. The practical difficulty of evaluating the sensitivity matrix at the unknown "true values" $\underline{\theta}_o$ and σ_o is overcome by using the estimates $\hat{\underline{\theta}}$ and $\hat{\sigma}$. However, fundamental difficulties lie in what is meant by the "true" values of the parameters, and how the confidence regions derived from the normal distribution of $\hat{\underline{\theta}}$ are to be interpreted.

The probability distribution for $\hat{\underline{\theta}}$ is in terms of hypothetical "true" values $\underline{\theta}_o$. When some physical constant is being estimated, with the variation in the estimates being due to measuring inaccuracies, the concept of the true value is valid and understandable as that which would have been obtained in the absence of errors. However, it is

impossible to define what is meant by $\underline{\theta}_o$ in the structural identification application where the parameters refer to a model which is just an approximate and simplified description of the real structural dynamics. For example, the assumption of a time-invariant linear model is clearly shown to be incorrect by the changes in the optimal value of the parameters estimated from successive segments of the strong-motion records. For some of the parameters, especially the modal periods, these changes are much greater than the error bounds calculated for the individual short segments or the overall records. In such circumstances, the concept of true parameter values is meaningless.

The second fundamental difficulty is in interpreting what is meant by the distribution for $\hat{\underline{\theta}}$. In the classical approach, the concept of probability is usually related to a measure of long-run proportion, and the distribution refers to the values of $\underline{\theta}$ which would be found in repetitive trials. In structural identification from earthquake records, and many other applications of parameter estimation, there is not the luxury of repeated experiments. There is a unique set of records, and what is required is the capability to make valid inferences about the model parameters $\underline{\theta}$ from a single set of samples $\underline{x}$, without the interpretation having to resort to the concept of a repetition of hypothetical random experiments which cannot be performed.

These problems of interpretation can be overcome by taking a Bayesian approach. In Bayesian statistics, probability is interpreted as a measure of the plausibility of some proposition on the basis of specific information, which may consist of observational data and assumptions. The propositions may refer to observable events, but they

may also refer to hypotheses about the parameters of a model, for example. The classical interpretation of probability as frequency in the long run is not required. As will be shown below, the distribution of $\underline{\theta}$ can be defined directly in terms of estimates $\hat{\underline{\theta}}$ from a single set of data, with no need to resort to the artifice of repeated experiments.

In the Bayesian approach, the posterior probability density $p(\underline{\theta},\sigma|\underline{x})$ for the parameter vector $\underline{\theta}$ and the error variance σ^2 is proportional to the product of the prior probability density $p(\underline{\theta},\sigma)$ and the likelihood function $p(\underline{x}|\underline{\theta},\sigma)$ as used earlier. By Bayes' rule,

$$p(\underline{\theta},\sigma|\underline{x}) = \frac{p(\underline{x}|\underline{\theta},\sigma)p(\underline{\theta},\sigma)}{p(\underline{x})} \tag{16}$$

The marginal distribution of $\underline{x}$,

$$p(\underline{x}) = \int_{\underline{\theta},\sigma} p(\underline{x}|\underline{\theta},\sigma)p(\underline{\theta},\sigma)d\underline{\theta}d\sigma \tag{17}$$

does not depend on the parameters. If a uniform prior distribution is taken, $p(\underline{\theta},\sigma)$ is also independent of the parameters, so

$$p(\underline{\theta},\sigma|\underline{x}) = cp(\underline{x}|\underline{\theta},\sigma) \tag{18}$$

where c is not dependent on $\underline{\theta}$ or σ. (For a uniform prior, the range of the allowable parameters must be kept finite to ensure finite integrals.)

In the Bayesian approach, one can choose the maximum a posteriori (MAP) estimates which maximize $p(\underline{\theta},\sigma|\underline{x})$ as representing the most plausible estimates given the data $\underline{x}$. Equation (18) shows that for the

uniform prior the MAP estimates are the maximum likelihood estimates, and hence with Gaussian modelling of the errors they are also the least-squares output-error estimates.

The distribution $p(\underline{\theta},\sigma|\underline{x})$ in terms of $J(\underline{\theta})$ is

$$p(\underline{\theta},\sigma|\underline{x}) = \frac{c}{(2\pi\sigma^2)^{N/2}} \exp\left[-\frac{1}{2\sigma^2} J(\underline{\theta})\right] \tag{19}$$

Thus, the MAP estimates are the optimal estimates $\hat{\sigma}^2 = \frac{1}{N} J(\hat{\underline{\theta}})$, and $\hat{\underline{\theta}}$ which minimizes $J(\underline{\theta})$.

Consider now an expansion of $p(\underline{\theta},\hat{\sigma}|\underline{x})$ about the optimal parameter values $\hat{\underline{\theta}}$, remembering $\hat{\underline{\theta}}$ is defined by $\frac{\partial J(\hat{\underline{\theta}})}{\partial\underline{\theta}} = \underline{0}$.

$$
\begin{aligned}
p(\underline{\theta},\hat{\sigma}|\underline{x}) &= \frac{c}{(2\pi\hat{\sigma}^2)^{N/2}} \exp\left\{-\frac{1}{2\hat{\sigma}^2}\left[J(\hat{\underline{\theta}}) + (\underline{\theta}-\hat{\underline{\theta}})^T \frac{\partial J(\hat{\underline{\theta}})}{\partial\underline{\theta}}\right.\right. \\
&\qquad \left.\left. + \frac{1}{2}(\underline{\theta}-\hat{\underline{\theta}})^T \frac{\partial^2 J(\hat{\underline{\theta}})}{\partial\underline{\theta}^2}(\underline{\theta}-\hat{\underline{\theta}}) + \ldots\right]\right\} \\
&\simeq p(\hat{\underline{\theta}},\hat{\sigma}|\underline{x}) \exp\left\{-\frac{1}{4\hat{\sigma}^2}(\underline{\theta}-\hat{\underline{\theta}})^T \frac{\partial^2 J(\hat{\underline{\theta}})}{\partial\underline{\theta}^2}(\underline{\theta}-\hat{\underline{\theta}})\right\} \tag{20}
\end{aligned}
$$

This has the form of a multidimensional Normal distribution with mean $\hat{\underline{\theta}}$ and covariance matrix $\hat{S}^{-1}$, where the sensitivity matrix $\hat{S}$ is given by:

$$\hat{S}_{ij} = \frac{1}{2\hat{\sigma}^2} \frac{\partial^2 J(\hat{\underline{\theta}})}{\partial\theta_i \partial\theta_j}$$

$$= \frac{N}{2J(\hat{\underline{\theta}})} \frac{\partial^2 J(\hat{\underline{\theta}})}{\partial\theta_i \partial\theta_j} \qquad (21)$$

The second derivative matrix of J is given by:

$$\frac{\partial^2 J(\hat{\underline{\theta}})}{\partial\theta_i \partial\theta_j} = 2 \sum_{n=1}^{N} \left\{ \frac{\partial m(t_n|\hat{\underline{\theta}})}{\partial\theta_i} \frac{\partial m(t_n|\hat{\underline{\theta}})}{\partial\theta_j} - [x_n - m(t_n|\hat{\underline{\theta}})] \frac{\partial^2 m(t_n|\hat{\underline{\theta}})}{\partial\theta_i \partial\theta_j} \right\} \qquad (22)$$

In practice, the relatively small second term is neglected in the calculation of the sensitivity matrix (it would be zero if the model fitted the data exactly). Thus the expression used to calculate the covariance matrix of the parameters is identical to that determined by the maximum likelihood approach:

$$\hat{S}_{ij} = \frac{N}{J(\hat{\underline{\theta}})} \sum_{n=1}^{N} \frac{\partial m(t_n|\hat{\underline{\theta}})}{\partial\theta_i} \frac{\partial m(t_n|\hat{\underline{\theta}})}{\partial\theta_j} \qquad (23)$$

However, the multidimensional Normal distribution is now for $\underline{\theta}$ about the known $\hat{\underline{\theta}}$, while previously it was for $\hat{\underline{\theta}}$ in repeated sampling of $\underline{x}$ about the hypothetical and unknown $\underline{\theta}_o$. Note that it is now exact to evaluate the sensitivity matrix at $(\hat{\underline{\theta}}, \hat{\sigma})$ while previously it was evaluated at this parameter state as an approximation to the required evaluation at $(\underline{\theta}_o, \sigma_o)$.

The covariance matrix should be interpreted as indicating the precision with which the values of the parameters are specified by the data, rather than as a measure of the error about "true values" which

cannot be defined. The change in the optimal values of the parameters between different segments of the data because of changes in the structural system during the response may considerably exceed the standard error for the different segments, showing the inappropriateness of the concept of true parameter values for a model which is merely an approximation to the actual system.

The precision of the parameter vector $\underline{\theta}$ as a whole may be studied using the full posterior density for $\underline{\theta}$ given by equation (20). The multidimensional normal distribution of the vector containing K parameters leads to confidence regions at level $\gamma = 1-\alpha$ of the form

$$(\underline{\theta}-\hat{\underline{\theta}})^T \hat{S}(\underline{\theta}-\hat{\underline{\theta}}) \leq \chi^2_{K;\alpha} \tag{24}$$

where $\chi^2_{K;\alpha}$ is the value of the K degree of freedom chi-squared variable which has probability α of being exceeded. Typically α is chosen as 0.1, 0.05 or 0.01. The inequality defines a hyper-ellipse centered at $\hat{\underline{\theta}}$ in the K-dimensional parameter space.

Some of the parameter estimates will be poor if the $\hat{S}$ matrix is ill-conditioned, in which case the hyper-ellipse will be very elongated in particular directions. A fast check for the possible near singularity of $\hat{S}$, without calculating its eigenvalues, is to calculate the ratios, η_i, of the diagonal elements to the largest diagonal element $\hat{S}_{kk}$, and the interaction coefficients ρ_{ij}:

$$\eta_i = \hat{S}_{ii}/\hat{S}_{kk} \quad , \quad \hat{S}_{kk} = \text{maximum diagonal element of } \hat{S} \tag{25}$$

$$\rho_{ij} = -\hat{S}_{ij}/[\hat{S}_{ii}\hat{S}_{jj}]^{\frac{1}{2}} \tag{26}$$

If an η_i is nearly zero or a $|\rho_{ij}|$ is nearly unity, $\hat{S}$ is ill-conditioned. The case where η_i is zero means J is not dependent on the ith parameter, while when $|\rho_{ij}|$ is unity the ith and jth sensitivity coefficients are linearly dependent, i.e.

$$\frac{\partial m(t_n|\underline{\theta})}{\partial \theta_i} = K \frac{\partial m(t_n|\underline{\theta})}{\partial \theta_j} \qquad \text{for all } t_n \tag{27}$$

When sensitivity coefficients are linearly dependent, the parameters cannot be estimated uniquely as there is some line in the $\underline{\theta}$ space along which J does not vary, i.e., the estimates of the parameters are coupled. For the linear structural models, estimates of the damping and participation factor of the same mode are often nearly coupled. The reason for this is that the resonant amplification of a mode depends on the ratio of the participation factor to the damping factor, and most of the contribution of a mode to the response comes from frequencies close to its resonance. Thus the two individual parameters can be varied without greatly affecting the calculated response provided their ratio is kept constant.

To obtain numerical values for the precision of the parameter estimates, it is simpler to consider the marginal posterior density for each component θ_i separately, rather than the confidence region for the complete $\underline{\theta}$ vector. These distributions are Normal with mean $\hat{\theta}_i$ and standard error

$$\Lambda_i = [\hat{S}^{-1}]^{1/2}_{ii} \tag{28}$$

When there is no interaction between parameters, i.e., all $\rho_{ij} = 0$ for $j \neq i$, or if the interaction is neglected, then:

$$\Lambda_i = [\hat{S}_{ii}]^{-1/2} \qquad \text{(interaction neglected)} \tag{29a}$$

Often there is significant interaction only between pairs of parameters, as for example the damping and participation factor of the same mode as discussed above. In that case, where only the jth parameter interacts with the ith,

$$\Lambda_i = [\hat{S}^{-1}]^{1/2}_{ii} = [(1-\rho^2_{ij})\hat{S}_{ii}]^{-1/2} \tag{29b}$$

so the standard error is increased by the factor

$$\frac{1}{[1-\rho^2_{ij}]^{1/2}}$$

over what it would have been in the absence of interaction.

Note that although the time-domain version of J has occurred explicitly in the development given here, in the previous section it was stated through an appeal to Parseval's theorem that the time-domain and frequency-domain versions are exactly equivalent if all the frequency points are used and practically equivalent if the frequency band used in the identification includes all the significant response. Thus the results for the sensitivity of the parameter estimates are equally

applicable to the time-domain and frequency-domain identification techniques.

The number to be used for N (the number of data points) in the frequency-domain evaluation of $\hat{S}_{ij}$ is the number of time-domain points used to calculate the FFTs, not the reduced number of frequency-domain points in the identification bandwidth. The use of only some of the frequency-domain points in the evaluation of J and its second derivative matrix is only for computational efficiency. Provided the frequency band containing all the significant response is included, the values of J and $\partial^2 J/(\partial\theta_i\partial\theta_j)$ are virtually identical to those obtained from using all the frequency points, as has been verified by calculation in a few cases. In using only the 9.5 Hz band from 0.5 to 10 Hz, for example, in the study of JPL Building 180 response instead of the full-band from 0 to 25 Hz, which gives almost exactly the same values for the parameter estimates and J and its second derivative matrix, the computational efficiency should not be penalized by reducing the sensitivity matrix by a factor of 9.5/25, or increasing the standard errors by $[25/9.5]^{1/2}$.

The results of this section can be applied to system identification in general. The only requirement is that the errors are modelled as Gaussian. The form of the system model, as opposed to the white noise statistical model for the errors, has not been involved in the error analysis, and enters only at the evaluation stage for finding the minimum of J and calculating the sensitivity matrix.

3.4 Selection of the Number of Modes

The minimization of the output error produces the optimal model containing a given number of modes. As more modes are added, the error J at the optimal parameter estimates decreases. However, beyond a few modes the decrease in J with an additional mode becomes slight. Often the parameters for the additional mode are physically unreasonable or their standard errors are large, and the identification algorithm may fail to converge because the output error is insensitive to the parameters of the extra mode. Some method is required to determine the optimal trade-off between the closeness-of-fit of the model to the data and the number of parameters required to represent the model.

The concept of the optimal or "correct" number of modes is ill-defined. For a synthesized example where the response was generated for a system with ten well-separated modes, and then the excitation and calculated response used to identify the known system, only six modes could be identified because the other four modes made an insignificant contribution to the response. In such circumstances, the criterion for selecting the number of modes can at best indicate whether the additional mode makes a significant reduction in the error, as the true number of modes cannot be determined when some modes make little contribution to the response. With continuous linear structural systems, the true number of modes is infinite, but in typical earthquake response only very few, less than a dozen, make a significant contribution to the response. Since it is impossible to identify all modes, some criterion is required for determining whether a new mode which is identified is important.

The choice of how many modes to include can be made subjectively, of course, and this is what was done in our earlier studies. An upper limit on the number of modes which could be included was imposed by the practical difficulties of obtaining convergence of the iterative identification algorithms. However, the number of modes for which good parameter estimates were obtained was usually felt to be one or two less than the maximum number which could be identified. Consequently, it would be useful to have a set criterion for determining the "optimal" number of modes.

One possible criterion for producing a trade-off between the closeness-of-fit to time-series data and the number of parameters in the model has been suggested by Akaike [1]. Akaike's information criterion (AIC) takes the form of an extension of the maximum likelihood method. Instead of __maximizing__ the likelihood function $p(\underline{x}|\underline{\theta},K)$, where K indicates the number of parameters to be estimated in the vector $\underline{\theta}$, he __minimizes__

$$AIC(\underline{\theta},K) \;=\; -2 \, \log \, p(\underline{x}|\underline{\theta},K) + 2K \tag{30}$$

as a function of both $\underline{\theta}$ and K. With the Gaussian noise model, this becomes:

$$AIC(\underline{\theta},\sigma,K) \;=\; N \, \log \, (2\pi\sigma^2) + \frac{1}{\sigma^2} \, J(\underline{\theta}) + 2K \tag{31}$$

Thus, for a given number of parameters K, the optimal parameter estimates are the maximum likelihood ones, but the AIC also provides a basis for comparing the maximum likelihood models with different numbers

of parameters. As more parameters are added to the model, $p(\underline{x}|\underline{\theta},K)$ increases, decreasing the first term in the AIC, but the second term increases, so that a minimum of the AIC occurs at some optimal number of parameters $\hat{K}$. If two models had the same goodness-of-fit as given by $J(\hat{\underline{\theta}})$, the AIC selects the one with fewer parameters, in agreement with the principle of parsimony; in fact the model with more parameters must decrease J significantly before it becomes preferred. Hipel [11] has presented a number of applications of AIC to geophysical data which demonstrates its effectiveness in model building.

The AIC can be interpreted in the Bayesian approach by replacing the uniform prior distribution $p(\underline{\theta},\sigma)$ by one in which the prior probability for a model with K parameters is proportional to e^{-K}. This particular weighting is obviously arbitrary – any monotonically decreasing function for positive K would satisfy the principle of parsimony that a model with fewer parameters is to be preferred. An obvious generalization is to make the weighting $e^{-\beta K}$, where β is a positive constant, in which case K is replaced by βK in the AIC. The larger β the greater the preference for few parameters.

For the models considered here, the number of parameters $K = 5R+1$ when there are R modes. Substituting the expressions found earlier for $\hat{\underline{\theta}}$ and $\hat{\sigma}^2$, and dropping constant terms, the optimal number of modes $\hat{R}$ by the Akaike criterion is that which minimizes

$$AIC(R) = N \log J(\hat{\underline{\theta}}_R) + 10R \qquad (32)$$

There are N data points to be fitted, and $\hat{\underline{\theta}}_R$ denotes the optimal parameter vector for R modes.

4. IDENTIFICATION STUDIES

4.1 Identification with the Unshifted Records

The initial identification studies of the behavior of JPL Building 180 in the San Fernando earthquake as reported by Beck [2] and McVerry [12] and summarized in this section used the standard unshifted records [7]. The studies in the time domain considered the first 20 seconds of the S82E records, performing acceleration, velocity and displacement matches, while the frequency-domain method was applied to the first 40.96 seconds of both horizontal components but was restricted to acceleration matching. The variation with time of the effective linear parameters was investigated in both studies by considering sub-intervals of these segments. The results for the segment from 0 to 20 seconds are given in this section, in particular noting some problems with the values estimated for some of the higher mode parameters. The parameter values given in this section, while minimizing the error criterion for the original records, are not the best estimates possible from the earthquake records; the optimal values presented in section 4.3 based on the synchronized records are certainly more realistic.

The one-, two- and three-mode models of JPL Building 180 identified from the first 20 seconds of the unshifted S82E longitudinal components of the San Fernando records are listed in Table 2a. Most of the frequency-domain identifications were performed over the band 0.50 Hz to

TABLE 2

IDENTIFIED PARAMETER VALUES FROM THE SAN FERNANDO RECORDS
S82E COMPONENT (0-20 SECONDS)

(a) Unshifted Records

No. of Modes	Quantity Matched	Mode r	T_r (sec)	ζ_r (%)	c_r	$\sum c_r$	J
1	Displacement	1	1.27	2.0	0.9	0.9	0.106
	Velocity	1	1.26	2.6	1.1	1.1	0.131
	Acceleration	1	1.26	3.5	1.3	1.3	0.350
	Acceleration Spectrum (0.5-10.0 Hz)	1	1.26	3.5	1.3	1.3	0.336
2	Velocity	1	1.26	2.5	1.00	0.48	0.097
		2	0.35	14.0	−0.52		
	Acceleration	1	1.25	4.2	1.50	1.03	0.148
		2	0.37	13.0	−0.47		
	Acceleration Spectrum (0.5-10.0 Hz)	1	1.25	4.2	1.48	1.01	0.142
		2	0.37	13.1	−0.47		
3	Velocity	1	1.262	2.4	1.01	0.33	0.087
		2	0.383	5.0	−0.22		
		3	0.308	8.8	−0.46		
	Acceleration	1	1.251	4.3	1.50	0.86	0.106
		2	0.380	5.5	−0.25		
		3	0.298	11.1	−0.39		
	Acceleration Spectrum (0.73-5.81 Hz)	1	1.253	4.2	1.48	0.84	0.100
		2	0.381	5.4	−0.24		
		3	0.299	11.5	−0.40		

TABLE 2 (CONT.)

(b) Aligned Records

No. of Modes	Quantity Matched	Shift n	Mode r	T_r (sec)	ζ_r (%)	c_r	$\sum c_r$	J
1	Acceleration Spectrum (0.5-10.0 Hz)	-2	1	1.239	4.1	1.56	1.56	0.291
2	Acceleration spectrum (0.5-10.0 Hz)	3	1	1.271	3.8	1.28	0.80	0.073
			2	0.405	7.8	-0.48		
	Acceleration Spectrum (0.73-5.80 Hz)	3	1	1.270	3.7	1.27	0.79	0.070
			2	0.405	7.8	-0.48		
3	Velocity	6	1	1.287	3.4	1.14	1.09	0.020
			2	0.429	7.8	-0.51		
			3	0.342	20.3	0.46		
	Velocity	4	1	1.277	3.2	1.13	0.90	0.025
			2	0.414	7.2	-0.43		
			3	0.257	9.2	0.20		
	Acceleration	4	1	1.276	3.6	1.22	1.01	0.0491
			2	0.414	7.5	-0.47		
			3	0.255	12.0	0.26		
	Acceleration Spectrum (0.5-10.0 Hz)	4	1	1.276	3.6	1.22	1.01	0.0487
			2	0.414	7.4	-0.46		
			3	0.255	11.8	0.25		
	Acceleration Spectrum (0.73-5.80 Hz)	4	1	1.277	3.6	1.24	1.04	0.0475
			2	0.414	7.6	-0.47		
			3	0.255	12.8	0.27		

TABLE 2(b) (CONT.)

No. of Modes	Quantity Matched	Shift n	Mode r	T_r (sec)	ζ_r (%)	c_r	$\sum c_r$	J
4	Acceleration	4	1	1.2765	3.57	1.22	0.97	0.0478
				±0.0007	±0.08	±0.02		
			2	0.4141	7.6	-0.47		
				±0.0005	±0.2	±0.01		
			3	0.253	14.3	0.30		
				±0.002	±1.4	±0.02		
			4	0.178	5.9	-0.08		
				±0.003	±2.4	±0.02		
	Acceleration Spectrum (0.5-10 Hz)	4	1	1.2765	3.56	1.21	0.95	0.0475
				±0.0006	±0.05	±0.01		
			2	0.4142	7.5	-0.465		
				±0.0004	±0.1	±0.005		
			3	0.254	13.4	0.28		
				±0.002	±0.6	±0.01		
			4	0.177	5.0	-0.07		
				±0.003	±1.3	±0.01		
5	Acceleration	4	1	1.2765	3.57	1.22	0.98	0.0477
				±0.0007	±0.08	±0.02		
			2	0.4141	7.6	-0.47		
				±0.0005	±0.2	±0.01		
			3	0.253	14.4	0.30		
				±0.002	±1.4	±0.02		
			4	0.177	7.3	-0.09		
				±0.003	±3.0	±0.03		
			5	0.129	1.8	0.02		
				±0.002	±2.3	±0.02		
5	Acceleration Spectrum (0.5-10 Hz)	4	1	1.2765	3.58	1.21	0.98	0.0474
				±0.0006	±0.05	±0.01		
			2	0.4141	7.5	-0.465		
				±0.0004	±0.1	±0.005		
			3	0.254	13.7	0.28		
				±0.002	±0.6	±0.01		
			4	0.177	5.5	-0.08		
				±0.003	±1.3	±0.01		
			5	0.140	17	0.03		
				±0.014	±9	±0.03		

10.0 Hz, while the Nyquist frequency was 25 Hz. Note that for a model with a given number of modes, the agreement between the parameter values estimated from the time-domain and frequency-domain matching of the acceleration response is excellent. However, the estimates of the damping factors and participation factors from the different response quantities in the time domain are not in good agreement.

There are problems with the estimates of the parameters for the third mode. The identified period of 0.30 seconds (3.3 Hz) lies in a trough of the Fourier amplitude spectrum of the acceleration response, and does not correspond to a significant peak of the transfer function (Figures 2 and 3). The closest peak of the acceleration spectrum is at 3.9 Hz, corresponding to the period of 0.26 seconds used as the initial estimate in the optimization algorithms. The participation factor also has the opposite sign to that expected. It takes a value of −0.39, compared to +0.24 for Wood's model or +0.25 for a uniform shear beam.

There are other problems with the estimates from the unshifted records. The participation factor at the roof must be greater than one for the first mode, as can be seen from equation (4) bearing in mind that the mode shape increases monotonically with height; in fact it is 1.27 for a uniform shear beam and 1.30 for the partial-composite model. The values from the displacement and velocity matches, which are less than or close to unity, are therefore suspect. A related point is that the sum over all the modes of the participation factors at any location should equal unity. For the roof, the participation factor decreases as the mode number increases at a fairly rapid rate (it is proportional to $\frac{1}{2n-1}$ for the nth mode of a uniform shear beam), and the sum for even the

first few modes should be close to unity. For a uniform shear beam, the sum of the roof participation factors for the first three modes is 1.10, while it is 1.08 for Wood's model. The values of 0.86 for the three-mode acceleration fit, and more particularly 0.33 for the velocity fit, are much smaller than expected.

The S08W transverse response was studied much less extensively than the S82E motion. Only the frequency-domain method was used for this component. The estimated parameter values, Table 3a, are not so obviously dubious as those for the third mode in the S82E direction. However, the participation factor and damping of the second mode appear unusually high. The parameter values were also at greater variance with Wood's values than for the other direction.

4.2 Synchronizing Earthquake Records

During the early studies discussed in the last section, it was speculated that the unrealistic values obtained for some of the parameters might have been caused by nonlinearities in the response. At the time, there were no grounds to suspect nonsynchronization of the records, particularly since the accelerographs were interconnected to give a common time-base.

However, in later work considering earthquake records from the Vogel Building, Wellington, New Zealand [5,14], the prospect arose of a time-shift between the digitized records from different locations in the structure because of difficulties in determining common time-marks at the beginning of the original film records. A straightforward application of the frequency-domain identification technique to the records

TABLE 3

IDENTIFIED PARAMETER VALUES FROM THE SAN FERNANDO RECORDS

S08W COMPONENT

(a) Unshifted Records (0-40 Seconds)

No. of Modes	Quantity Matched	Mode r	T_r (sec)	ζ_r (%)	c_r	$\sum c_r$	J
3	Acceleration Spectrum (0.27-5.86 Hz)	1	1.420	6.5	1.49	1.04	0.232
		2	0.401	12.0	-0.76		
		3	0.207	10.0	0.31		

(b) Aligned Records (0-40 seconds)

No. of Modes	Quantity Matched	Shift n	Mode r	Estimates ± Standard Errors				
				T_r(sec)	ζ_r(%)	c_r	$\sum c_r$	J
3	Acceleration Spectrum (0.27-5.86 Hz)	2	1	1.434	5.1	1.44	1.11	0.180
			2	0.436	8.4	-0.58		
			3	0.233	6.4	0.25		
4	Acceleration Spectrum (0.27-5.86 Hz)	3	1	1.436	4.4	1.35	0.84	0.164
			2	0.444	6.0	-0.54		
			3	0.240	7.0	0.26		
			4	0.178	8.0	-0.23		
	Acceleration Spectrum (0.25-10 Hz)	3	1	1.437 ±0.002	4.4 ±0.1	1.36 ±0.015	0.94	0.184
			2	0.443 ±0.001	5.9 ±0.2	-0.53 ±0.01		
			3	0.2405 ±0.0005	6.8 ±0.2	0.255 ±0.007		
			4	0.180 ±0.001	5.0 ±0.5	-0.15 ±0.01		

TABLE 3 (CONT.)

(c) Aligned Records (0-20 seconds)

No. of Modes	Quantity Matched	Shift n	Mode r	Estimates ± Standard Errors				
				T_r(sec)	ζ_r(%)	c_r	$\sum c_r$	J
3	Acceleration Spectrum (0.25-10 Hz)	2	1	1.430 ±0.003	4.8 ±0.2	1.42 ±0.02	1.06	0.198
			2	0.436 ±0.002	8.5 ±0.4	-0.59 ±0.015		
			3	0.2336 ±0.0007	5.8 ±0.3	0.23 ±0.01		
4	Acceleration Spectrum (0.25-10 Hz)	3	1	1.433 ±0.002	4.2 ±0.2	1.36 ±0.02	0.93	0.178
			2	0.444 ±0.001	5.7 ±0.3	-0.53 ±0.015		
			3	0.2404 ±0.0008	6.6 ±0.3	0.25 ±0.01		
			4	0.180 ±0.025	4.7 ±0.6	-0.15 ±0.015		

from two earthquakes produced unrealistic parameter estimates and poor
matching for the second mode in the mid-height and roof records, despite
this mode showing up clearly as peaks in the Fourier amplitude spectra
at the modal period measured in vibration tests. Because of the
suspected lack of synchronization of the records, some experimentation
was carried out on shifting the excitation and response records integral
numbers of timesteps (0.02 seconds) with respect to each other. The
identifications were repeated for different shifts, allowing the
measure-of-fit to be minimized with respect to the shift as well as the
modal parameters. This led to excellent results at the optimal time-
shifts, with the normalized measure-of-fit for one of the components
being the best yet achieved by the authors for an essentially full-
duration record. Furthermore, the optimal shifts of each of the
response records with respect to the basement record were consistent in
that they differed at most by one timestep for those components recorded
in the same accelerograph, but were different for the various accelero-
graphs.

One consequence of the shifting of the mid-height record in Vogel
Building relative to the basement record was that the effective partici-
pation factor of the second mode, which was estimated as -0.34 from the
unshifted record, became +0.36 when the optimal shift was used. The
negative value from the unshifted records was unrealistic, since the
value calculated from the known mass distribution and the second mode-
shape measured in forced-vibration tests was positive. This wrong sign
for the effective participation factor recalled the previous
difficulties in estimating the parameters of the third longitudinal mode

of JPL Building 180. The almost correct magnitude but wrong sign of the mid-height, second-mode participation factor for Vogel Building was consistent with the optimal time-shift of 0.10 seconds, corresponding to a phase error of 180° at the second mode period of 0.20 seconds (the phase change at frequency f from a time-shift $n\Delta t$ is $360 fn\Delta t$ degrees).

These considerations suggested that it might be worthwhile to re-examine the JPL Building 180 records with time-shifts, even though they were supposedly synchronized. As described in the remainder of this paper, the optimal time-shift strategy overcame the problems associated with the estimates of the higher mode parameters, and produced improved measures-of-fit. It is concluded that the basement and roof records [7] are unsynchronized by about 0.08 seconds.

Discussions with Dr. A. G. Brady and Professor D. E. Hudson lead us to believe that this is due to the digitizing process where the origin of time was selected as the start of the light traces of the accelero-graph record. Any difference between the start-up times of the film transporting mechanisms would mean that this choice of time origin must lead to some lack of synchronization, even if the instruments are triggered simultaneously as intended. It would perhaps be better when digitizing the film records to choose the position of the time origin by ensuring that the first time mark away from the beginning of the light traces is assigned the same time value for each record (time marks on the RFT-250 instruments installed in the JPL Building 180 are at 0.5 second intervals). This recommendation is based on the reasonable assumption that the differences in time for each instrument to produce the timing mark corresponding to a common timing pulse is much less than

the differences in the time to accelerate the film in each accelerograph to its operating speed.

If the above explanation regarding the lack of synchronization of the JPL Building 180 records is correct, other sets of digitized building records may suffer from a similar defect. Fortunately, it should be possible to synchronize the records, at least in the absence of structural damage, by making the relative time-shift another unknown parameter to be estimated in the system identification, as we have done in this study.

4.3 Identification with the Optimally Shifted Records

The estimation of the modal parameters of JPL Building 180 from the San Fernando earthquake records was repeated treating the shift between the records as another parameter to be estimated. The shift which gave the best measure-of-fit for acceleration is interpreted as that which correctly synchronizes the basement and roof records.

For the longitudinal (S82E) direction, the segment from 0 to 20 seconds was studied extensively using both the time-domain and frequency-domain methods. The models were built up one mode at a time. In the frequency-domain study, the initial estimates of the parameters for the new mode were taken as the values for Wood's partial-composite model with 5% damping, while for the other modes they were the optimal estimates for the model containing one fewer mode. For the time-domain identifications, the required initial estimates were the periods, taken as Wood's values, and the damping factors, taken as 5% of critical. The optimal estimates for models with different numbers of modes, estimated

by matching the acceleration spectrum, acceleration, velocity or displacement at the roof, are given in Table 2b. The velocity matches achieved by the optimal models from the frequency-domain acceleration identifications are shown in Figures 4a and b for the unshifted and shifted records respectively. Figures 5a, b and c compare the measured response with that of the optimal three-mode model determined from the synchronized acceleration time histories.

In Table 2b, the shifts between the records are indicated as multiples of the digitized record time-step of 0.02 seconds. A positive shift of n time-steps means that point i on the original response record corresponds to point i+n on the basement record, that is, the records are synchronized by discarding the first n points of the basement record. For the acceleration and acceleration-transform matches the results are given for the optimal shifts. For the velocity matches the results are given for the shifts which are optimal for each of the velocity and the acceleration.

A comparison of the parameter estimates derived from the original unshifted records and the optimally synchronized records for the S82E direction reveals several important changes (Table 2).

The first point to note is the effect that the synchronization has had on the third-mode parameters, whose questionable values in the original studies prompted this re-investigation. The new third- mode period estimate of 0.255 seconds (3.92 Hz) corresponds to a peak of the Fourier amplitude spectrum of the acceleration response (Figure 3) and agrees closely with Wood's synthesized value of 0.257 seconds and his

Fig. 4a. Comparison of the measured (———) and optimal 3-mode model (– – –) relative velocities, S82E component. The model was identified from the Fourier spectra of the unshifted acceleration records.

Fig. 4b.   Comparison of the measured (——) and optimal 3-mode model (– – –) relative velocities, S82E component. The model was identified from the Fourier spectra of the shifted acceleration records.

Fig. 5a. Comparison of the measured (——) and optimal 3—mode model
(- - -) relative displacements, S82E component. The model was
identified from the optimally synchronized acceleration
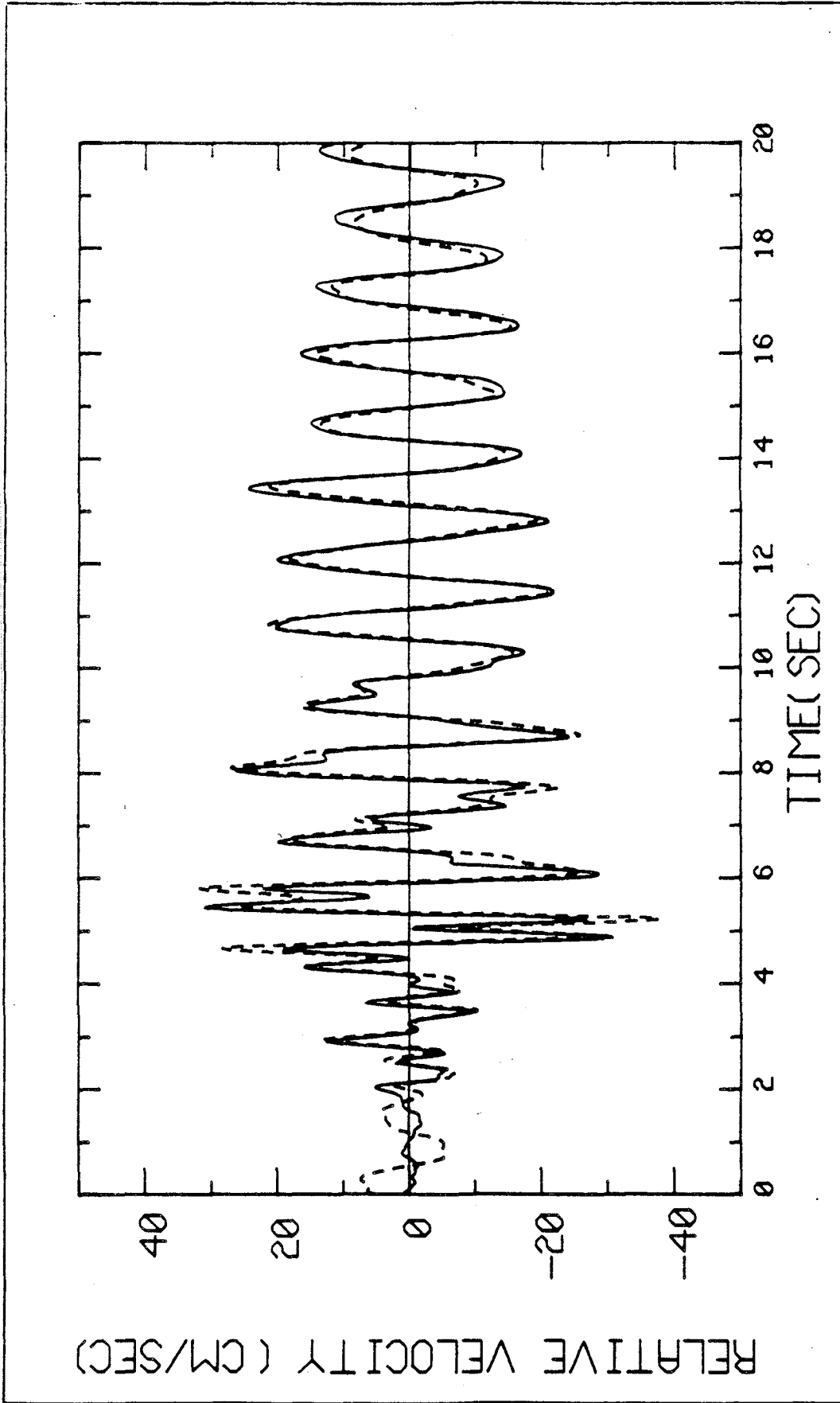records.

Fig. 5b.   Comparison of the measured (——) and optimal 3-mode model
           (- - -) relative velocities, S82E component. The model was
           identified from the optimally synchronized acceleration
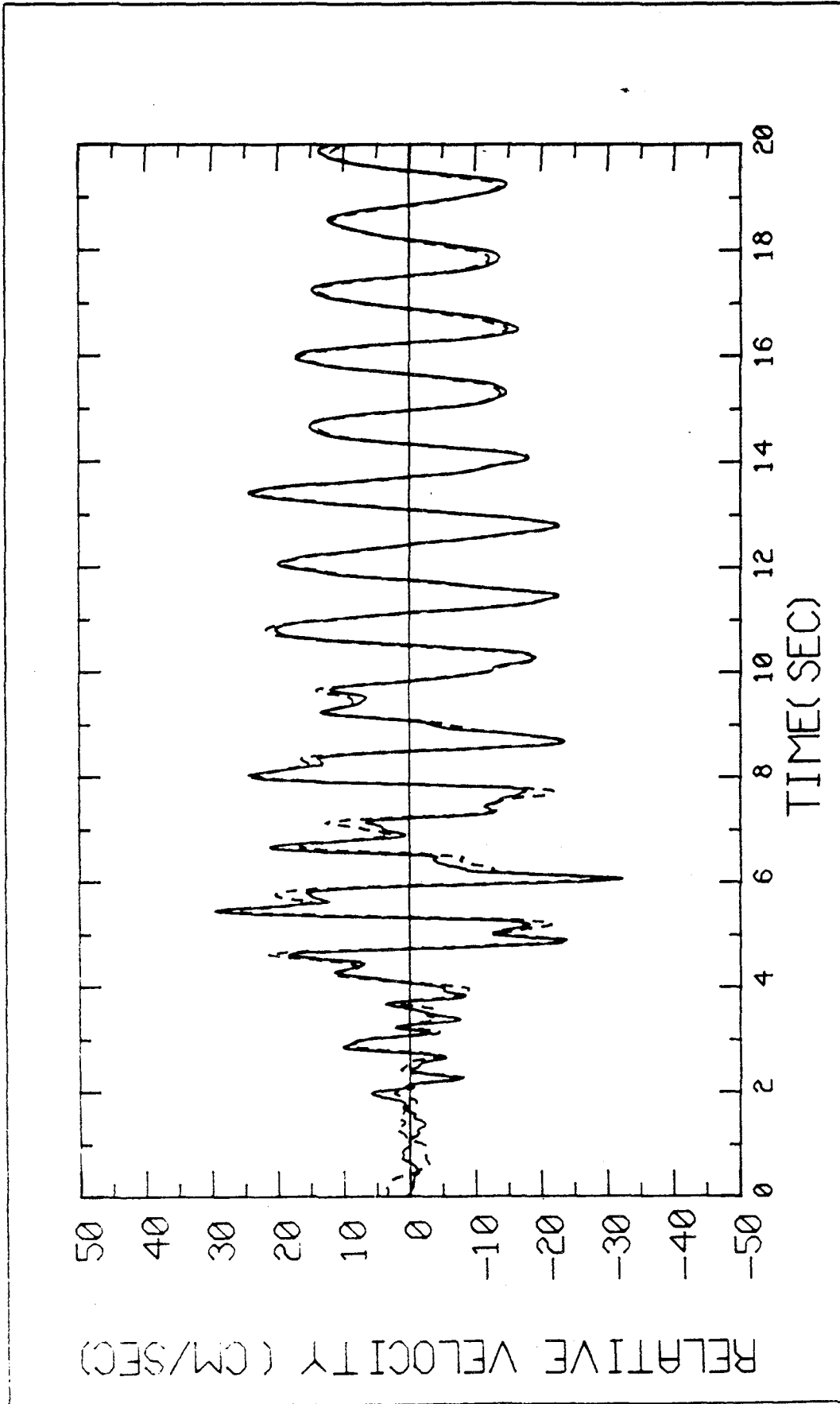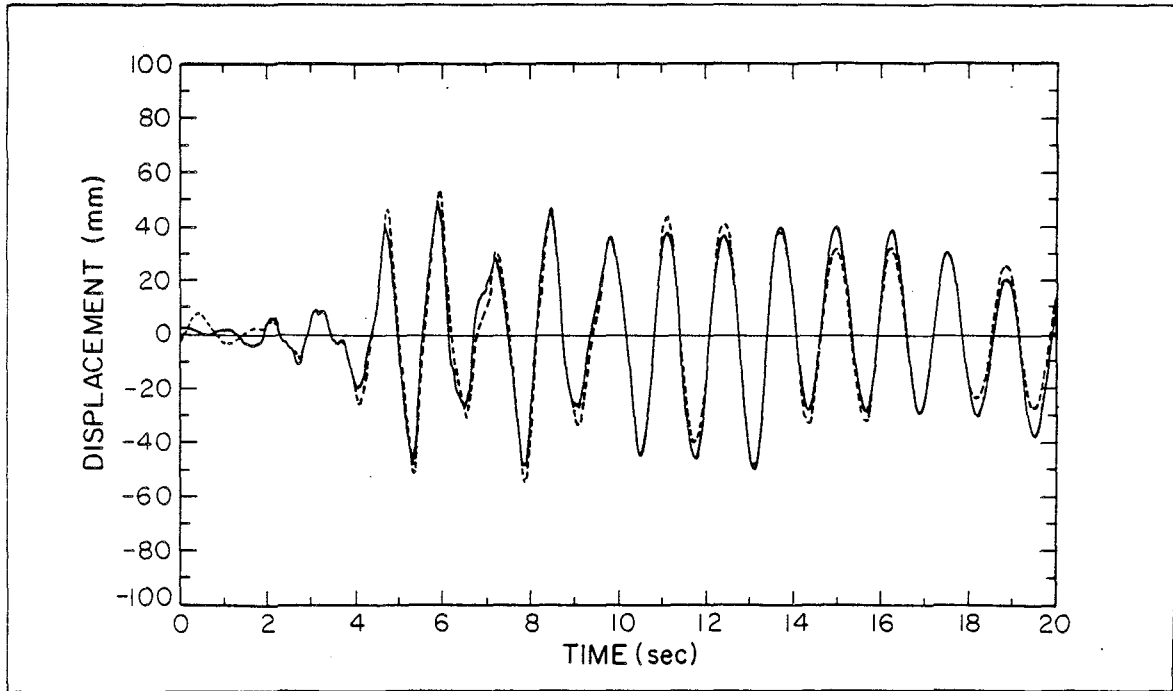   records.

Fig. 5c. Comparison of the measured (———) and optimal 3-mode model
          (- - -) relative accelerations, S82E component. The model was
          identified from the optimally synchronized acceleration
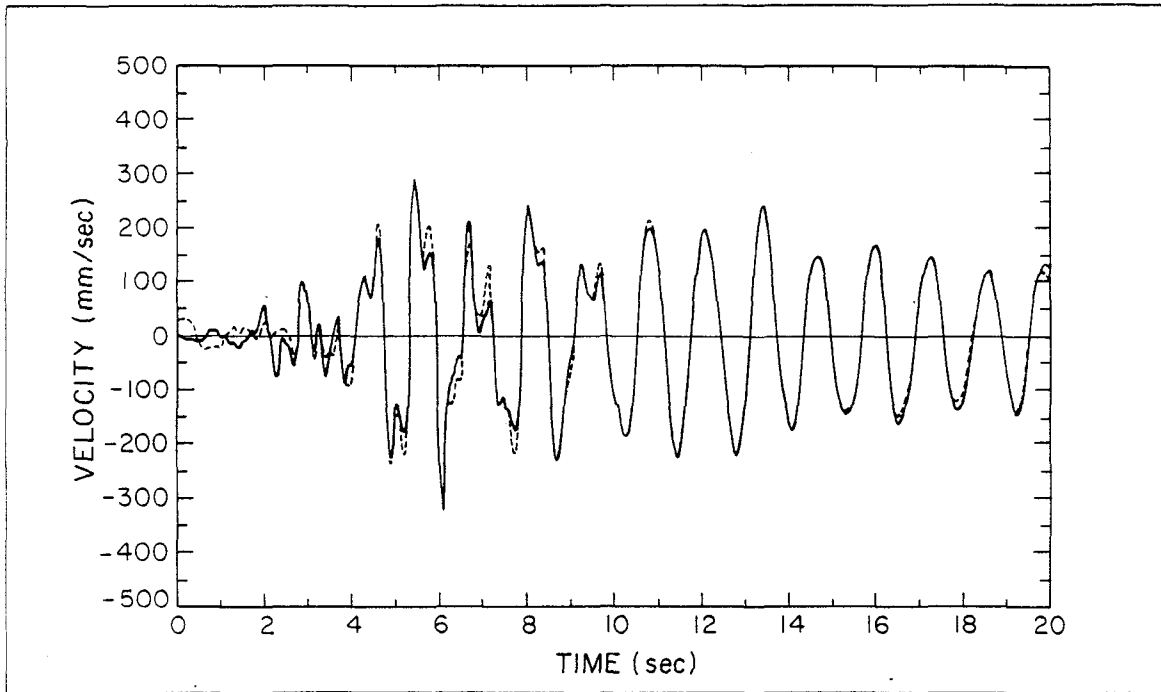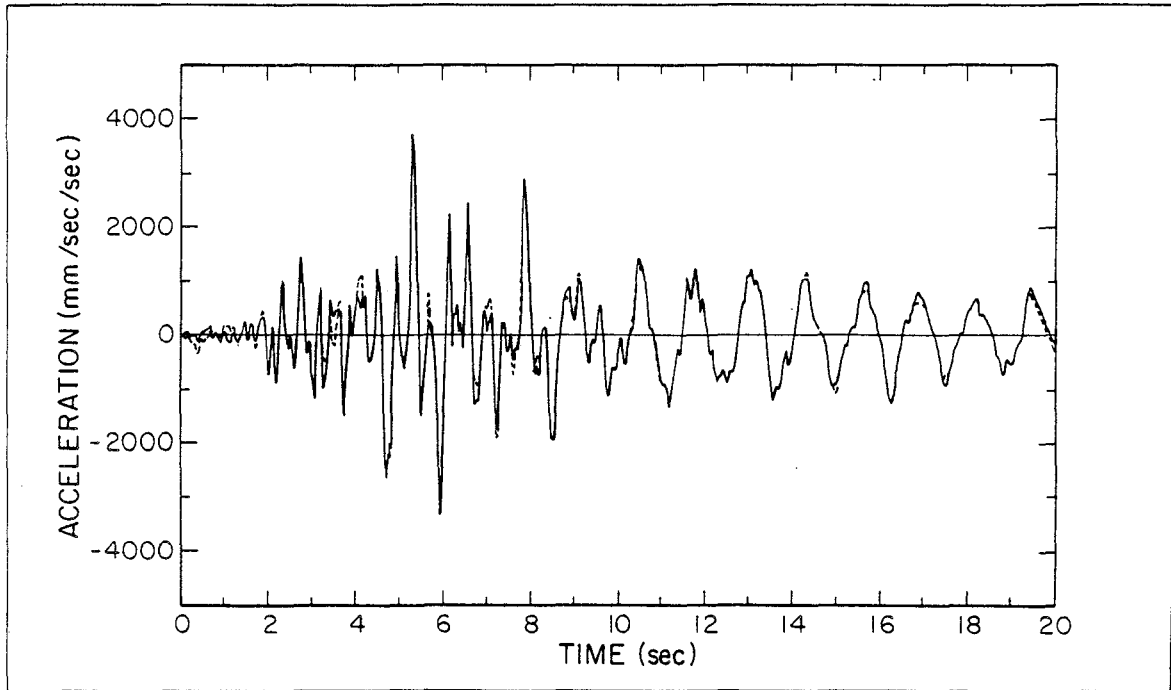   records.

adjusted value of 0.260 seconds. The original estimate of 0.299 seconds
(3.34 Hz) from the unshifted records, identified using the same initial
estimate as for the shifted records, lay in a trough of the Fourier
amplitude spectrum and did not coincide with any of the modes of the
synthesized models. Similarly, the estimated participation factor now
takes on a realistic value. It has the correct sign and its value of
between 0.25 and 0.30 for the various models is in good agreement with
the synthesized value of 0.24.

The values estimated for the participation factors of the other
modes have also changed significantly. The first-mode participation
factor has reduced from 1.48 to 1.22, compared with Wood's synthesized
value of 1.30, while the second-mode participation factor has changed
from -0.24 to -0.47, in agreement with the synthesized value. The sum
of the participation factors also lies much closer to unity than pre-
viously; 1.01 for the three-mode model and 0.98 for the five- mode
model, as against 0.84 for the three-mode model identified from the
original unshifted records.

Another feature is that more modes have now been identified.
Misalignment of the records has greater effect at higher frequencies, as
a time-shift of $n\Delta t$ modifies the Fourier transform at frequency f by the
factor $e^{i2\pi f n\Delta t}$, that is, changes the phase by 360 $f n\Delta t$ degrees. As the
estimation of the parameters of each mode is governed mainly by the
response near the modal frequency, the identification of the higher
modes is affected more by the phase corruption. At least four modes

have now been identified with physically reasonable parameter values,
while previously the identifications were suspect beyond two modes.

The synchronization has led to much reduced errors J at the optimal
shifts for each number of modes. As the higher modes could not be
matched well previously because of the corruption of the phases around
their modal frequencies, addition of extra modes produced only modest
reductions in the error.

For the acceleration and acceleration-transform matches, the
optimal shifts agree within one time-step for the two-, three-, four-
and five-mode models, with a value of four time-steps or 0.08 seconds.
Velocity matching with a three-mode model gave an optimal time-shift of
six time-steps. However, the shift of 0.08 seconds is considered more
likely to be the correct one since the acceleration has stronger signals
for the higher modes, which are more sensitive to the effects of lack of
synchronization. Furthermore, the velocity records are likely to con-
tain correlated "measurement" errors arising from the integration of the
noise in the acceleration records which could contribute to the
discrepancies. When the optimal acceleration shift of four timesteps is
used for the velocity matching, increasing the measure-of-fit J_v to
0.025 from the value of 0.020 for the optimal velocity shift of six
timesteps, parameter values in good agreement with those estimated from
the acceleration are obtained. This is in contrast to the results from
the unshifted records, which showed considerable discrepancy between the
estimates from velocity and acceleration matching (Table 2a).

The variation with time of the effective linear models over the first 40 seconds of the response was investigated by using the frequency-domain method to identify the optimal two- and three-mode models for a series of segments of the records (Figure 6). Although sufficient segments were studied to trace the variations in the parameters, this aspect of the study was less extensive than that performed for the unshifted records [12].

The most noticeable variation in the parameters for the longitudinal direction was the lengthening of the fundamental period over the first ten seconds of the response, up to the time of the largest motion. The first-mode period changed from 1.02 seconds, close to the value of 0.99 seconds measured by Nielsen [16] in forced vibration tests during construction, to a maximum of 1.28 seconds during the largest amplitude response, before falling off slightly to 1.23 seconds over the last ten seconds of the analyzed record. The value identified for the overall response was 1.28 seconds, the same as for the strongest portion of the motion.

The second-mode period also varied during the response, and the values identified for various segments differed from those found from the unshifted records. A double peak around the second-mode frequency is one of the features of the Fourier spectrum of the east-west acceleration response (Figure 3). With the unshifted records, the identifications from the whole record (0-40 seconds), and also for the 0-20 second segment, produced a second-mode period of 0.38 seconds corresponding to the lower-amplitude peak, despite an initial estimate corresponding to the more dominant peak at 0.42 seconds which was chosen

JPL BUILDING 180 S82E. LONGITUDINAL RESPONSE SAN FERNANDO EARTHQUAKE

SEGMENT LENGTHS

× 20 seconds
+ 10 seconds
● 5 seconds
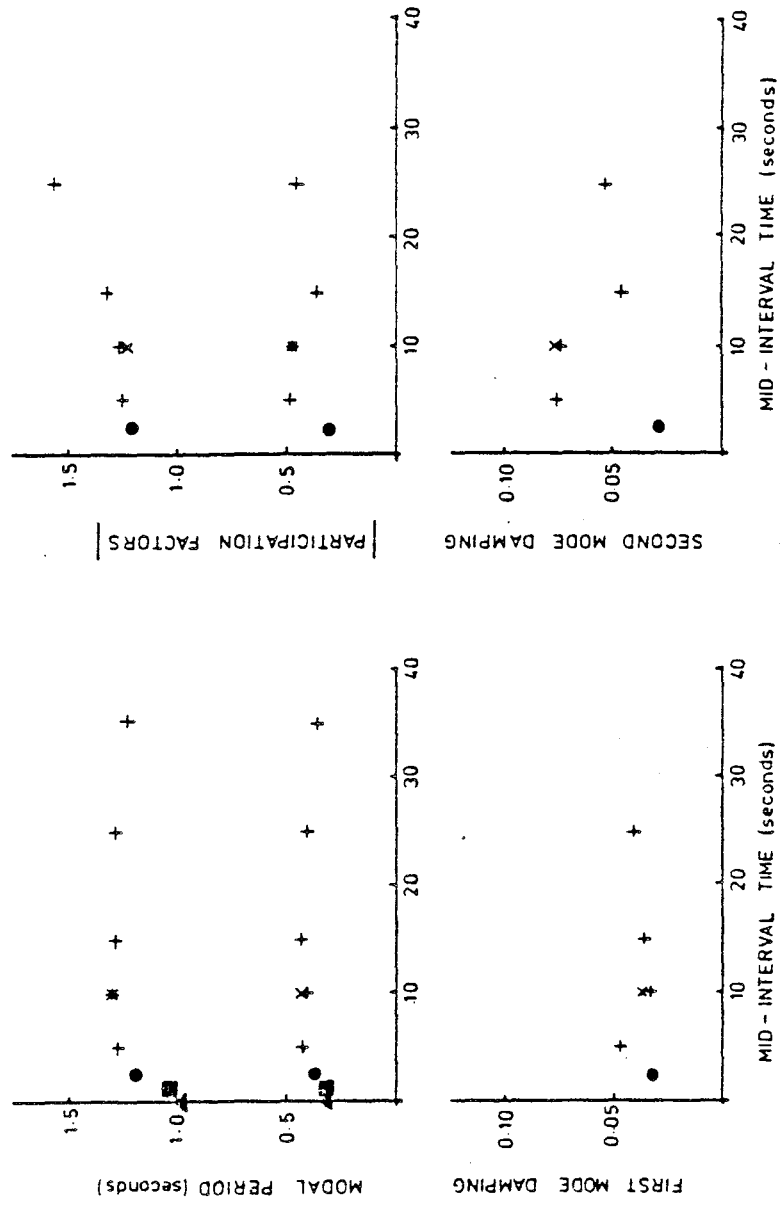■ 2.5 seconds
▲ pre-earthquake test

Fig. 6. Time variation of the parameters of linear models of JPL Building 180 identified in the frequency domain from segments of the optimally aligned San Fernando S82E records.

as the resonant period by Wood. The identification with the optimally aligned records produced an effective overall value of 0.414 seconds for the second mode period, in near agreement with Wood. However, there was a variation of the second-mode period with time which may have contributed to the double peak. For different segments of the records the identified value varied from 0.31 seconds at the beginning of the response to 0.42 seconds for the segment between 10 and 20 seconds before dropping to 0.39 seconds over the segment from 30 to 40 seconds. The initial value of 0.31 seconds may be compared with Nielsen's vibration test value of 0.33 seconds.

The values estimated for the modal dampings were rather different using the synchronized records than using the unshifted records, particularly for the initial portion of the response. Using the unshifted records, the identified dampings peaked at 15 and 12 percent for the first two modes about 3 seconds from the start of the records, before falling to values of 3.5 to 5.0 percent for the first mode, and 4.0 to 6.0 percent for the second mode, over the last twenty seconds. With the synchronized records, the dampings did not reach such large values early in the response. The peak values for the first two modes were only 4.5 and 7.5 percent, with the values later in the response similar to those estimated from the unshifted records.

For the 0 to 20 seconds segment, Akaike's information criterion (AIC) was applied to obtain a quantitative measure of the number of modes required to represent the response most parsimoniously in the sense of giving the best trade-off between the closeness of the fit and the number of parameters used in the model. Including more modes than

indicated by the AIC produces a marginal improvement in the measure-of-fit, but the estimates of additional parameters tend to be unreliable. The values summarized in Table 4 show that four modes provide the most parsimonious representation according to the AIC. This agreed with the intuitive feeling gained from examining the identification results produced by adding a fifth mode. For example, the parameter estimates from matching the acceleration history (time-domain method) and from matching the acceleration spectrum (frequency-domain method) are nearly identical for up to four modes in the models (Table 2b), but the two methods gave substantially different estimates for the fifth mode.

The standard errors are included with the parameter estimates in Table 2b for the four- and five-mode models, showing that the period estimates are the most precise, followed by the participation factors and dampings. Furthermore, the estimates of the first and second mode parameters are more precise than those of the higher modes. For the estimates from matching the acceleration histories, the standard errors were calculated using Eq. 28 which requires the inversion of the sensitivity matrix. On the other hand, the standard errors for the estimates from the acceleration spectrum were calculated using the simple approximation given by Eq. 29a. This approximation underestimates the standard errors for the damping and participation factors, primarily because of the interaction between these parameters (see, for example, Eq. 29b), but it produces satisfactory results for the period errors.

The normalized diagonal elements (Eq. 25) of the sensitivity matrix $\hat{S}$ for the four-mode model identified from the 0 to 20 seconds segment of the S82E records are given in Table 5, together with the corresponding

TABLE 4

A.I.C. VALUES FOR JPL BUILDING 180 S82E RESPONSE

Values of Akaike's information criterion (AIC) for the models identified from the optimally aligned acceleration records for the S82E motion of JPL Building 180. The models were identified from the Fourier acceleration spectra over the frequency band 0.5 to 10.0 Hz for the first 20 seconds of the motion. The minimum of AIC indicates that four modes provide the most parsimonious model.

$$AIC = N \log J + 2K$$
$$N = \text{number of data points} = 1024$$
$$K = \text{number of parameters (5 per mode)}$$

Modes	K	J	AIC
1	5	0.291	−1254
2	10	0.073	−2660
3	15	0.0487	−3065
4	20	0.0475	−3080
5	25	0.0474	−3072
6*	30	0.0469	−3073

*Nonsensical parameter values and non-convergence of algorithm for 6 modes.

interaction coefficients from the off-diagonal elements (Eq. 26). It can be seen that the interaction is insignificant except between the damping and participation factor of the same mode, with interaction coefficients of 0.68, 0.75, 0.82 and 0.68 for the first four modes.

Somewhat surprising in the original studies with the unshifted records was the extent of the interaction between the estimates of the modal frequencies and participation factors, particularly for some of the shorter segments. Unlike the interaction between the damping and participation factors, no simple explanation for this behavior is apparent. For example, for an identification performed for the 15-25 second interval over the 0.25 to 10 Hz band, the interaction coefficients between these parameters were 0.71 and 0.67 for the first two modes, greater than the values of 0.60 and 0.21 for the interactions between the estimates of the dampings and participation factors. Such high values for the interaction coefficients indicate that difficulties exist in extracting precise estimates of the parameters from the data, apparently caused by the phase distortion induced by the shift between the records. For the synchronized records, the interaction between the first two modal frequencies and participation factors is much reduced, to 0.47 and 0.11 for the 15-25 second interval.

As with the unshifted records, the response in the transverse (S08W) direction has been studied less extensively than the S82E component. Three- and four-mode models for the overall response (0 to 40 seconds) and the 0 to 20 second segment have been derived by the frequency-domain method, but the detailed temporal variation of the parameters has not been re-investigated. The results are presented in

TABLE 5

SENSITIVITY ANALYSIS FOR S82E RESPONSE (0-20 SECONDS)

The normalized diagonal elements η_i (Eq. 25) of the sensitivity matrix and the interaction coefficients ρ_{ij} (Eq. 26) for the off-diagonal elements of the sensitivity matrix. The only strong interaction is that between the damping and participation factor of each mode (shown underlined). The maximum diagonal element of the sensitivity matrix is $\hat{S}_{11} = 4.07 \times 10^6$.

	T_1	ζ_1	c_1	T_2	ζ_2	c_2	T_3	ζ_3	c_3	T_4	ζ_4	c_4
T_1	1.000	0.037	-0.16	-0.002	0.001	-0.004	0.000	0.000	-0.001	0.000	0.000	0.001
ζ_1		0.001	0.68	-0.001	-0.005	0.011	-0.003	0.002	-0.008	0.001	0.000	0.002
c_1			0.004	0.10	-0.056	0.24	-0.085	0.015	0.072	-0.029	0.031	-0.16
T_2				0.209	0.076	0.035	-0.066	-0.018	-0.076	0.003	0.005	0.016
ζ_2					0.001	0.75	0.044	-0.058	0.10	-0.012	0.000	-0.043
c_2						0.002	0.11	0.063	-0.024	0.025	-0.033	0.13
T_3							0.006	0.14	-0.086	-0.12	-0.008	-0.25
ζ_3								0.0001	0.82	0.041	-0.12	0.15
c_3									0.0002	0.082	0.12	0.076
T_4										0.001	0.057	-0.20
ζ_4											0.0000	0.68
c_4												0.0000

Table 3. Synchronizing the records has less dramatic effects than for the S82E direction, mainly because the original estimates were not so obviously in error. However, the new estimates agree much more closely with those of the synthesized models, and the models have been extended from three to four modes. The optimal timeshift for the S08W records is three timesteps or 0.06 second, compared with 0.08 second for the S82E records. This may be a consequence of the fact that the synchronization can only be achieved to within a timestep of 0.02 second.

For the first mode in the S08W direction, the estimates of the damping and participation factor have been reduced from the original values of 6.5% and 1.49 to 4.4% and 1.35 respectively from the synchronized records, more in agreement with Wood's values of 3% and 1.31. The changes have been larger for the second mode. The original period estimate of 0.401 seconds has become 0.444 seconds, closer to Wood's value of 0.436 seconds, while the high value of the damping and participation factors, 19% and −0.76, have been reduced to 6.0% and −0.54. The third- and fourth-mode periods and participation factors agree reasonably well with the synthesized values, but as with the lower modes the identified damping values are considerably higher than those Wood estimated from his study of the earthquake records.

The errors for the north-south models are larger than for the east-west models, and show less reduction with the synchronization of the records. This is caused partly by the relatively greater contribution of the higher modes not included in the models (i.e., beyond the fourth)

to the response than for the east-west direction, but may also be a reflection of a greater amount of nonlinear behavior.

The nonlinear behavior is revealed by the lengthening of the periods. The first mode period for the S08W direction increased by over sixty percent from the pre-earthquake vibration-test value, from 0.88 seconds to 1.44 seconds. The increase in the other direction was only about forty percent. The second-mode period also showed a considerable lengthening, from 0.29 to 0.44 seconds. The S08W response had a strong contribution from higher modes (shown by the high-frequency content of the acceleration time history of Figure 7a), each with time-varying properties, which produced poorer acceleration matches than for the other direction. However, the estimates of the parameters of the lower modes were sufficiently accurate to produce a good match of the velocity for which the high-frequency content was unimportant (Figure 7b).

The results of this study have been compared with those of Wood, and have in the main shown excellent agreement. From the success of Wood's study, it may appear that the trial-and-error approach is a satisfactory method for estimating the values of the structural parameters exhibited in measured earthquake response. However, the trial-and-error approach is a very lengthy procedure compared with computer optimization. Moreover, it must be stressed that Wood's study is one of the most successful of its type. Meticulous care was taken both in the initial synthesis of the model and in the adjustment to match the earthquake response. The agreement was considerably better than usually obtained by this type of approach. For example, Brandow and Johnston, who studied the building less extensively than Wood, did not achieve
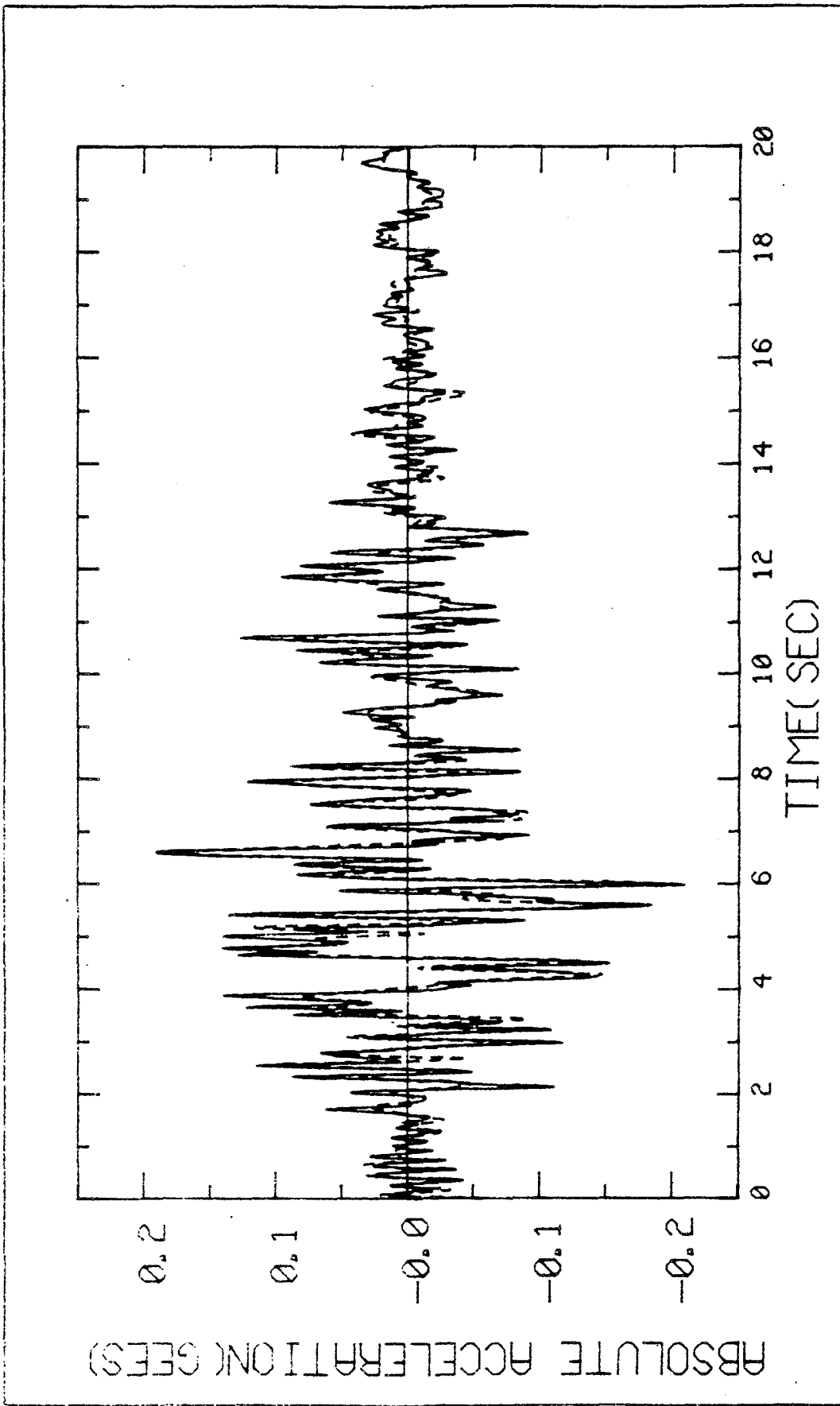
Fig. 7a. Comparison of the measured (———) and optimal 4-mode model (- - -) absolute accelera-
tions, S08W component. The model was identified from the Fourier spectra of the
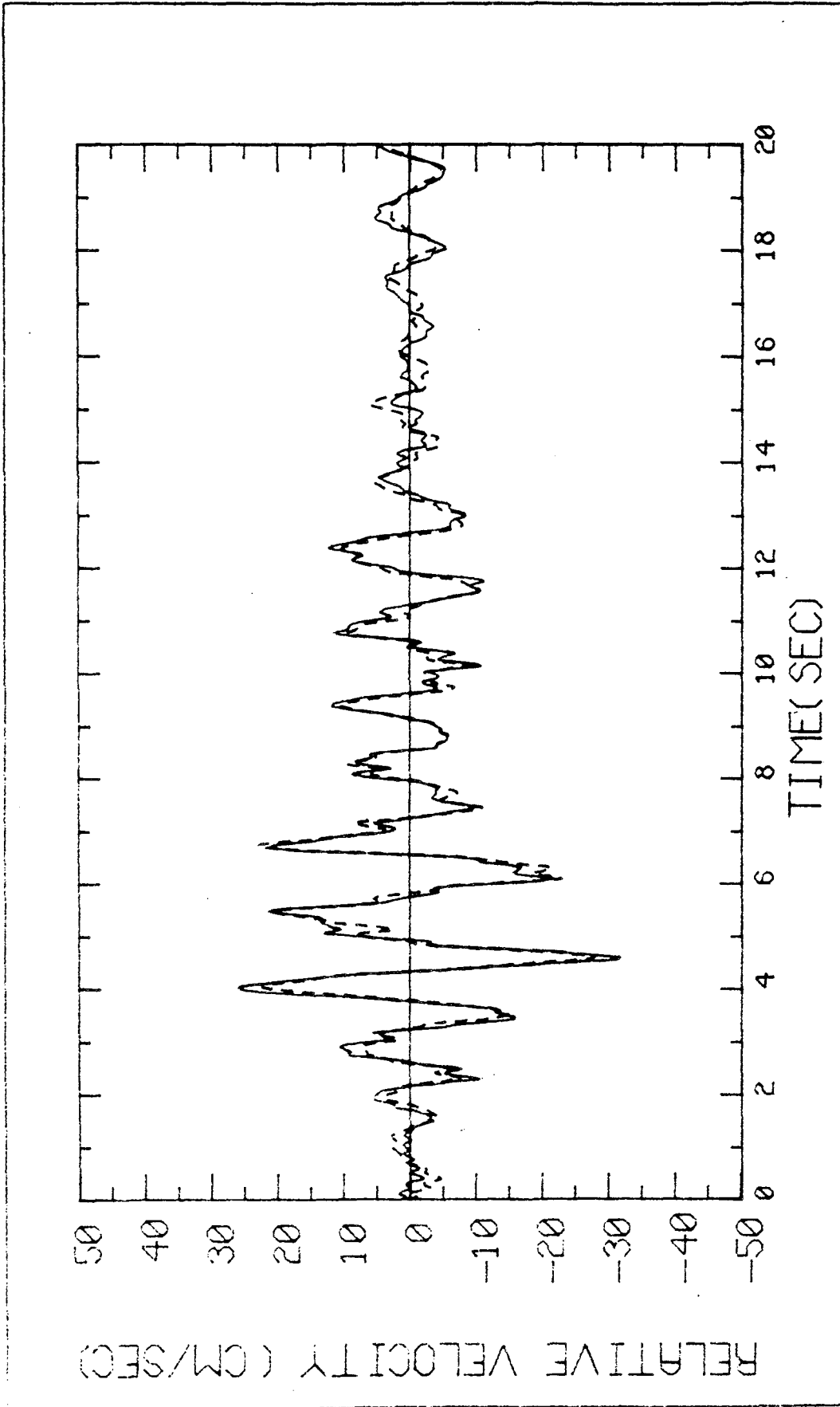optimally synchronized acceleration records.

Fig. 7b. Comparison of the measured (———) and optimal 4-mode model (— — —) relative velocities, S08W component. The model was identified from the Fourier spectra of the optimally synchronized acceleration records.

this level of agreement (Table 1). Furthermore, there were some
difficulties encountered by Wood in matching the Fourier amplitude spec-
tra of the acceleration responses. In particular, the resonant peaks of
the measured spectra were broader than those calculated for the models,
presumably because of the variation of the modal frequencies during the
response. Wood found the best matches of the overall spectra were
obtained by overestimating the peak amplitudes by about 30 percent. The
present systematic approaches automatically produce the parameter values
which best match the overall spectrum, and not just the peak values.
Wood also used the participation factors calculated from the synthesized
models, and estimated only the modal frequencies and dampings from the
earthquake records. The systematic approaches estimate all the parame-
ters from the records, although accuracy of the estimates of the damping
and participation factors is not high, primarily because of the interac-
tion between these parameters. The main source of error in Wood's
matches were offsets between the measured and model response (Figure 8a)
originally thought to be caused by slight overestimations of the funda-
mental periods, but more likely caused by the misalignment of the exci-
tation and response records revealed in the present study. This
conjecture is supported by Figure 8b, in which the response of Wood's
model has been calculated from the base excitation shifted forward with
respect to the roof record by 0.08 seconds, the optimal shift given by
the identification studies. As Wood's matches were based on only the
amplitude spectra, the phase distortions caused by the time-shift
between the records were not revealed in his frequency-domain matches.
However, probably the greatest disadvantage of a trial-and-error
approach to parameter estimation is that it is not known whether the

Fig. 8a.   Comparison of the measured (———) and model (- - -) relative velocities for Wood's refined 6-mode model, S82E direction.   The unshifted records were used.
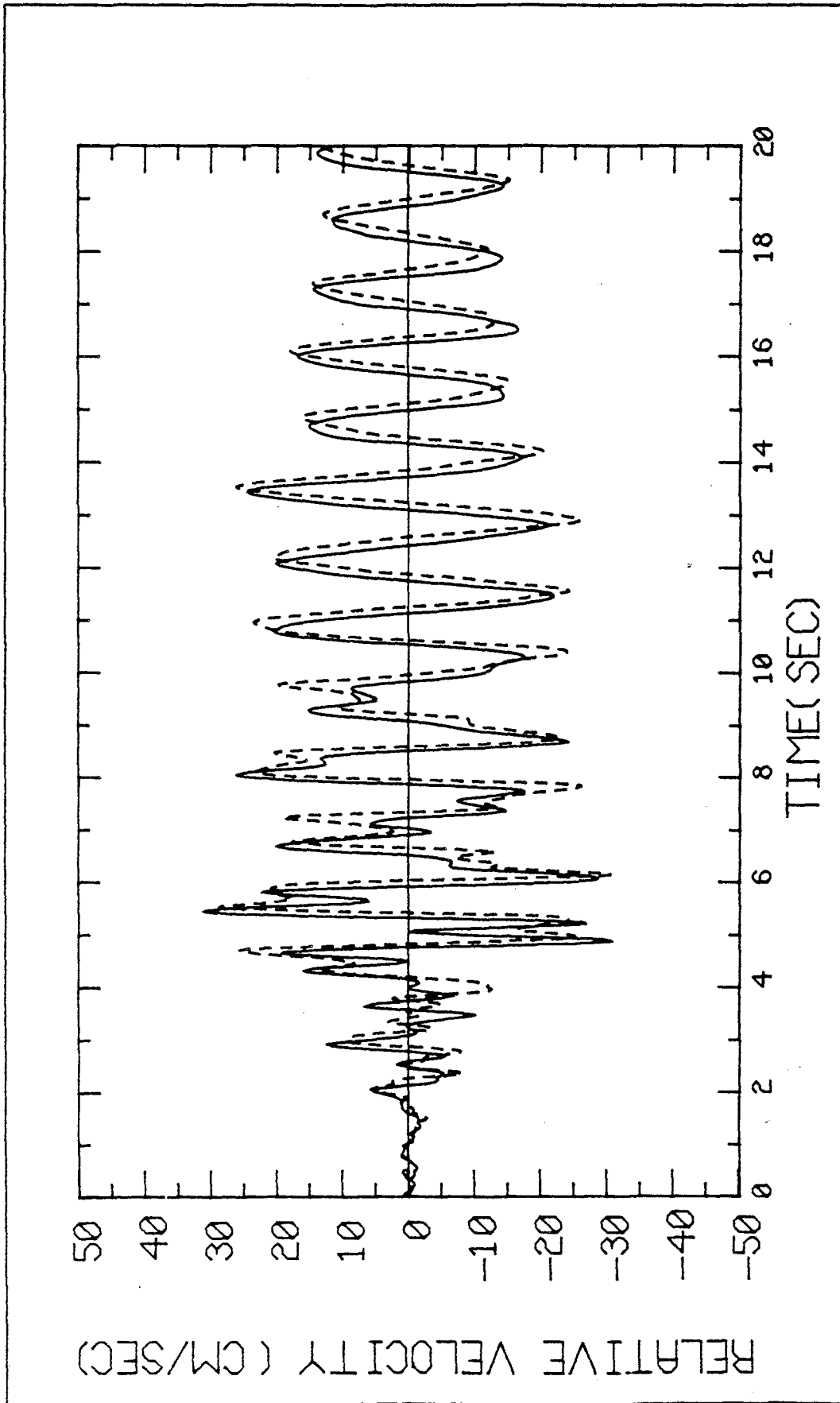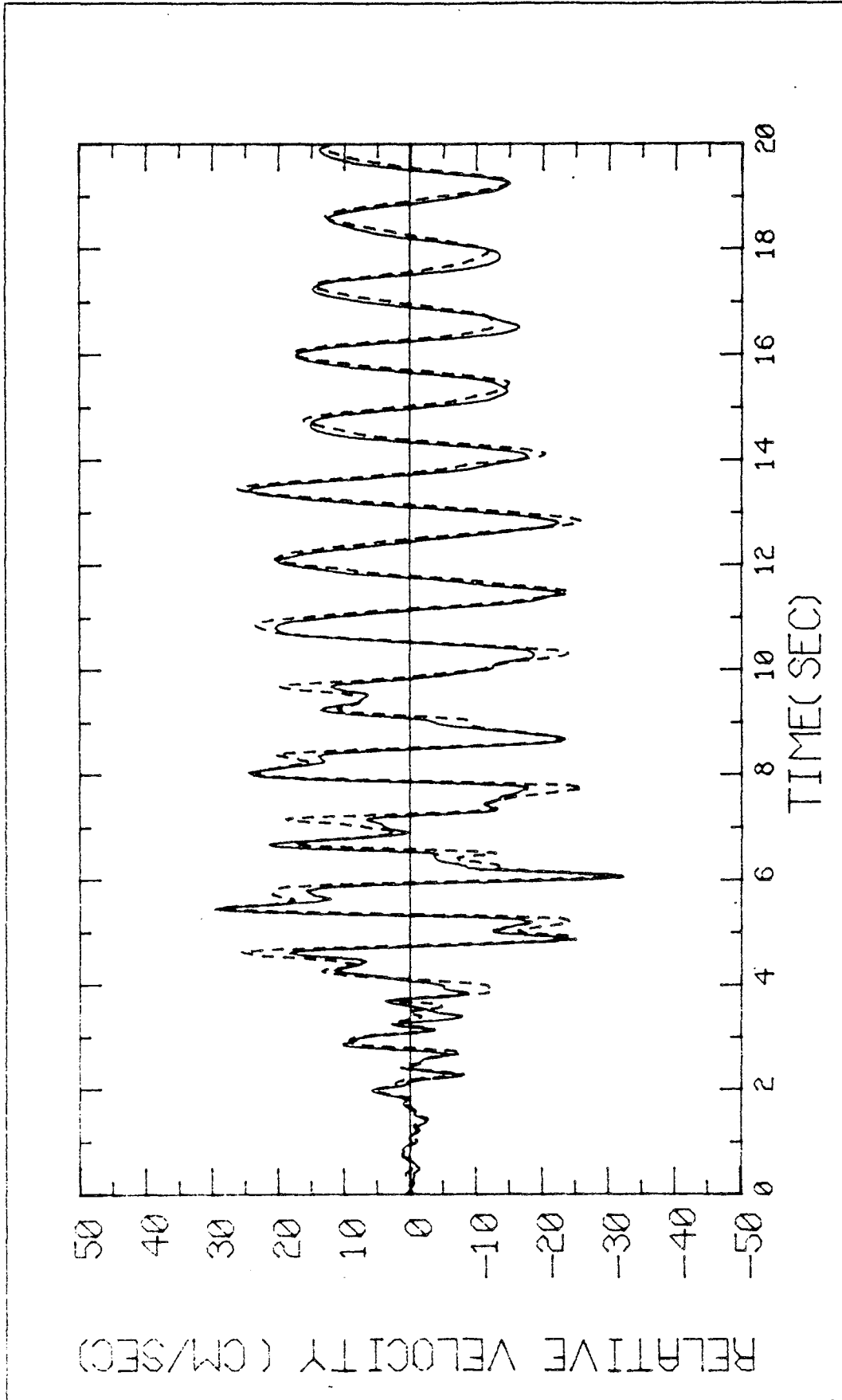
Fig. 8b. Comparison of the measured (———) and model (– – –) relative velocities for Wood's refined 6-mode model, S82E component. The basement record was shifted forward four timesteps (0.08 seconds) relative to the roof record. The better match compared with Fig. 8a, provides further evidence for the lack of synchronization of the original records.

best values have been found or, indeed, what the accuracy of the calculated estimates is likely to be. These problems are overcome by the systematic techniques discussed here.

5. CONCLUSIONS

Linear models of JPL Building 180 have been determined from the strong-motion records of its excitation and response in the 1971 San Fernando earthquake. Two systematic techniques provided estimates of the periods, dampings and participation factors of the dominant modes by the least-squares matching of the model and measured responses, one method operating in the time domain and the other in the frequency domain. Although the basement and roof accelerographs were interconnected, a previously undetected lack of synchronization of about 0.08 seconds between the two records has been revealed. Optimal alignment of the records led to significant improvements in the matches between the measured responses and those calculated for the identified models, and produced more reasonable estimates for the parameters of the higher modes. Earlier studies using the present identification techniques on the unshifted records [2,12] produced erroneous values for the estimates of the higher mode parameters because of the large phase distortions produced at the frequencies of these modes by the lack of synchronization.

It was found possible to determine time-invariant linear models appropriate for the overall response, and also to trace the temporal variation of the effective linear parameters due to nonlinear structural behavior. The values of the effective linear parameters varied signifi-

cantly, particularly up to the time of the largest motion. The fundamental periods in the longitudinal and transverse directions lengthened by about forty and sixty percent respectively, starting from values close to those measured in vibration tests. The second-mode periods lengthened considerably also. The effective periods were similar to those calculated by Wood for synthesized models which assumed cracking of the concrete encasing the steel columns. These synthesized models also indicated that the large period lengthenings were associated with a structure which approached but did not exceed yield. The effective viscous dampings were 3.6 and 4.4 percent of critical for the fundamental modes in the longitudinal and transverse directions, with values of around 5 and 7 percent during the maximum response.

Finally, the lack of precise synchronization exhibited by the records from JPL Building 180 may be a common feature of digitized film records from interconnected accelerographs. If so, the records must be synchronized to obtain reliable estimates of the parameters of the excited modes of a structure. The techniques discussed in this paper are apparently capable of achieving this synchronization to within one time-step of the digitized data, at least in the absence of structural damage where linear models have been found to give good reproductions of the recorded response. Furthermore, synchronization increases the number of modes for which the parameters can be estimated successfully. This represents a significant improvement in the amount of reliable information about structural behavior which can be extracted from strong-motion earthquake records, consequently increasing their

importance for monitoring structural performance during potentially

damaging motion.

REFERENCES

[1] Akaike, H., "A New Look at the Statistical Model Identification,"
     IEEE Trans. Auto. Control, AC-19, No. 6, 716-23, December 1974.

[2] Beck, J.L., Determining Models of Structures from Earthquake
     Records, Report EERL 78-01, California Institute of Technology,
     Pasadena, California, June 1978.

[3] Beck, J.L., "System Identification Applied to Strong Motion
     Records from Structures," in Earthquake Ground Motion and Its
     Effects on Structures, S.K. Datta (ed.), AMD-Vol. 53, ASME, New
     York, 1982.

[4] Beck, J.L. and P.C. Jennings, "Structural Identification Using
     Linear Models and Earthquake Records," Intl. J. Earthq. Engr. &
     Struc. Dyn., 8, 145-160, April 1980.

[5] Beck, J.L., P.M. Randall, and R.T. Hefford, Computer Analyses of
     New Zealand Earthquake Accelerograms, Physics and Engineering
     Laboratory, DSIR, Lower Hutt, New Zealand, 1981.

[6] Brandow and Johnston Associates, Design Analysis of the Jet
     Propulsion Laboratory, Building 180, prepared for the Jet Propul-
     sion Laboratory, California Institute of Technology, Pasadena,
     California, 1971.

[7] California Institute of Technology, Strong Motion Accelerograms,
     Vol. I-IV, Part G, Earthquake Engineering Research Laboratory,
     Pasadena, California.

[8] Foutch, D.A. and G.W. Housner, "Observed Changes in the Natural
     Periods of Vibration of a Nine Story Steel Frame Building," Proc.
     6th World Conf. Earthquake Eng., III, 2698-2704, New Delhi, India,
     January 1977.

[9] Foutch, D.A., G.W. Housner and P.C. Jennings, Dynamic Responses of
     Six Multistory Buildings during the San Fernando Earthquake,
     Earthquake Engineering Research Laboratory Report EERL 75-02,
     California Institute of Technology, Pasadena, California, October
     1975.

[10] Goodwin, G.C. and R.L. Payne, Dynamic System Identification:
     Experiment Design and Data Analysis, Academic Press, 1977.

[11] Hipel, K.W., "Geophysical Model Discrimination Using the Akaike
     Information Criterion," IEEE Trans. Auto. Control, AC-26, No. 2,
     358-78, April 1981.

[12]   McVerry, G.H., <u>Frequency Domain Identification of Structural Models from Earthquake Records</u>, Earthquake Engineering Research Laboratory, Report EERL 79-02, California Institute of Technology, Pasadena, California, October 1979.

[13]   McVerry, G.H., "Structural Identification in the Frequency Domain from Earthquake Records," <u>Intl. J. Earthq. Engr. & Struct. Dyn.</u>, 8, 161-180, April 1980.

[14]   McVerry, G.H., "Frequency Domain Structural Identification From Earthquake Records," in <u>Mathematics and Models in Engineering Science</u>, A. McNabb, R.A. Wooding & M. Rosser (eds.), 35-53, DSIR, Wellington, New Zealand, 1982.

[15]   Murphy, L.M. (ed.), <u>San Fernando, California, Earthquake of February 9, 1971</u>, U.S. Department of Commerce, National Oceanic and Atmospheric Administration (NOAA), Washington, D.C., 1973.

[16]   Nielsen, N.N., <u>Dynamic Response of Multistory Buildings</u>, Earthquake Engineering Research Laboratory, California Institute of Technology, Pasadena, California, June 1964.

[17]   Nigam, N.C. and P.C. Jennings, "Calculation of Response Spectra From Strong-Motion Earthquake Records," <u>Bull. Seism. Soc. Am.</u>, 59, 909-22, 1969.

[18]   Udwadia, F.E. and M.D. Trifunac, "Time and Amplitude Dependent Response of Structures," <u>Intl. J. Earthq. Engr. & Struct. Dyn.</u>, 2, 359-78, 1974.

[19]   Wood, J.H., <u>Analysis of the Earthquake Response of a Nine-Story Steel Frame Building during the San Fernando Earthquake</u>, Earthquake Engineering Research Laboratory, Report EERL 72-04, California Institute of Technology, Pasadena, California, 1972.

[20]   Wood, J.H., "Earthquake Response of a Steel Frame Building," <u>Intl. J. Earthq. Engr. & Struct. Dyn.</u>, 4, 349-77, 1976.

CALIFORNIA INSTITUTE OF TECHNOLOGY

Reports Published

by

Earthquake Engineering Research Laboratory*
Dynamics Laboratory
Disaster Research Center

Note: Numbers in parenthesis are Accession Numbers assigned by the
National Technical Information Service; these reports may be ordered
from the National Technical Information Service, 5285 Port Royal Road,
Springfield, Virginia, 22161. Accession numbers should be quoted on
orders for reports (PB --- ---). Reports without this information
either have not been submitted to NTIS or the information was not avail-
able at the time of printing. An N/A in parenthesis indicates that the
report is no longer available at Caltech.

1. Alford, J.L., G.W. Housner and R.R. Martel, "Spectrum Analysis of
   Strong-Motion Earthquakes," 1951. (Revised August 1964). (N/A)

2. Housner, G.W., "Intensity of Ground Motion During Strong Earth-
   quakes," 1952. (N/A)

3. Hudson, D.E., J.L. Alford and G.W. Housner, "Response of a Struc-
   ture to an Explosive Generated Ground Shock," 1952. (N/A)

4. Housner, G.W., "Analysis of the Taft Accelerogram of the Earth-
   quake of 21 July 1952." (N/A)

5. Housner, G.W., "A Dislocation Theory of Earthquakes," 1953. (N/A)

6. Caughey, T.K., and D.E. Hudson, "An Electric Analog Type Response
   Spectrum," 1954.(N/A)

7. Hudson, D.E., and G.W. Housner, "Vibration Tests of a Steel-Frame
   Building," 1954. (N/A)

8. Housner, G.W., "Earthquake Pressures on Fluid Containers," 1954.
   (N/A)

9. Hudson, D.E., "The Wilmot Survey Type Strong-Motion Earthquake
   Recorder," 1958. (N/A)

10. Hudson, D.E., and W.D. Iwan, "The Wilmot Survey Type Strong-Motion
    Earthquake Recorder, Part II," 1960. (N/A)

---

* To order directly by phone the number is 703-487-4650.

11. Caughey, T.K., D.E. Hudson, and R.V. Powell, "The CIT Mark II Electric Analog Type Response Spectrum Analyzer for Earthquake Excitation Studies," 1960. (N/A)

12. Keightley, W.O, G.W. Housner and D.E. Hudson, "Vibration Tests of the Encino Dam Intake Tower," 1961. (N/A)

13. Merchant, Howard Carl, "Mode Superposition Methods Applied to Linear Mechanical Systems Under Earthquake Type Excitation," 1961. (N/A)

14. Iwan, Wilfred D., "The Dynamic Response of Bilinear Hysteretic Systems," 1961. (N/A)

15. Hudson, D.E., "A New Vibration Exciter for Dynamic Test of Full-Scale Structures," 1961. (N/A)

16. Hudson, D.E., "Synchronized Vibration Generators for Dynamic Tests of Full-Scale Structures," 1962. (N/A)

17. Jennings, Paul C., "Velocity Spectra of the Mexican Earthquakes of 11 May and 19 May 1962," 1962. (N/A)

18. Jennings, Paul C., "Response of Simple Yielding Structures to Earthquake Excitation," 1963. (N/A)

19. Keightley, Willard O., "Vibration Tests of Structures," 1963. (N/A)

20. Caughey, T.K. and M.E.J. O'Kelly, "General Theory of Vibration of Damped Linear Dynamic Systems," 1963. (N/A)

21. O'Kelly, M.E.J., "Vibration of Viscously Damped Linear Dynamic Systems," 1964. (N/A)

22. Nielsen, N. Norby, "Dynamic Response of Multistory Buildings," 1964. (N/A)

23. Tso, Wai Keung, "Dynamics of Thin-Walled Beams of Open Section," 1964. (N/A)

24. Keightley, Willard O., "A Dynamic Investigation of Bouquet Canyon Dam," 1964. (N/A)

25. Malhotra, R.K., "Free and Forced Oscillations of a Class of Self-Excited Oscillators," 1964.

26. Hanson, Robert D., "Post-Elastic Response of Mild Steel Structures," 1965.

27. Masri, Sami F., "Analytical and Experimental Studies of Impact Dampers," 1965.

28. Hanson, Robert D., "Static and Dynamic Tests of a Full-Scale Steel-Frame Structure," 1965.

29. Cronin, Donald L., "Response of Linear, Viscous Damped Systems to Excitations Having Time-Varying Frequency," 1965.

30. Hu, Paul Yu-fei, "Analytical and Experimental Studies of Random Vibration," 1965.

31. Crede, Charles E., "Research on Failure of Equipment when Subject to Vibration," 1965.

32. Lutes, Loren D., "Numerical Response Characteristics of a Uniform Beam Carrying One Discrete Load," 1965. (N/A)

33. Rocke, Richard D., "Transmission Matrices and Lumped Parameter Models for Continuous Systems," 1966. (N/A)

34. Brady, Arthur Gerald, "Studies of Response to Earthquake Ground Motion," 1966. (N/A)

35. Atkinson, John D., "Spectral Density of First Order Piecewise Linear Systems Excited by White Noise," 1967. (N/A)

36. Dickerson, John R., "Stability of Parametrically Excited Differential Equations," 1967. (N/A)

37. Giberson, Melbourne F., "The Response of Nonlinear Multi-Story Structures Subjected to Earthquake Excitation," 1967. (N/A)

38. Hallanger, Lawrence W., "The Dynamic Stability of an Unbalanced Mass Exciter," 1967.

39. Husid, Raul, "Gravity Effects on the Earthquake Response of Yielding Structures," 1967. (N/A)

40. Kuroiwa, Julio H., "Vibration Test of a Multistory Building," 1967. (N/A)

41. Lutes, Loren Daniel, "Stationary Random Response of Bilinear Hysteretic Systems," 1967.

42. Nigam, Navin C., "Inelastic Interactions in the Dynamic Response of Structures," 1967.

43. Nigam, Navin C. and Paul C. Jennings, "Digital Calculation of Response Spectra from Strong-Motion Earthquake Records," 1968.

44. Spencer, Richard A., "The Nonlinear Response of Some Multistory Reinforced and Prestressed Concrete Structures Subjected to Earthquake Excitation," 1968. (N/A)

45. Jennings, P.C., G.W. Housner and N.C. Tsai, "Simulated Earthquake Motions," 1968.

46. "Strong-Motion Instrumental Data on the Borrego Mountain Earthquake of 9 April 1968," (USGS and EERL Joint Report), 1968.

47. Peters, Rex B., "Strong Motion Accelerograph Evaluation," 1969.

48. Heitner, Kenneth L., "A Mathematical Model for Calculation of the Run-Up of Tsunamis," 1969.

49. Trifunac, Mihailo D., "Investigation of Strong Earthquake Ground Motion," 1969. (N/A)

50. Tsai, Nien Chien, "Influence of Local Geology on Earthquake Ground Motion," 1969. (N/A)

51. Trifunac, Mihailo D., "Wind and Microtremor Induced Vibrations of a Twenty-Two Steel Frame Building," EERL 70-01, 1970.

52. Yang, I-Min, "Stationary Random Response of Multidegree-of-Freedom Systems," DYNL-100, June 1970. (N/A)

53. Patula, Edward John, "Equivalent Differential Equations for Nonlinear Dynamical Systems," DYNL-101, June 1970.

54. Prelewicz, Daniel Adam, "Range of Validity of the Method of Averaging," DYNL-102, 1970.

55. Trifunac, M.D., "On the Statistics and Possible Triggering Mechanism of Earthquakes in Southern California," EERL 70-03, July 1970.

56. Heitner, Kenneth Leon, "Additional Investigations on a Mathematical Model for Calculation of the Run-Up of Tsunamis," July 1970.

57. Trifunac, Mihailo D., "Ambient Vibration Tests of a Thirty-Nine Story Steel Frame Building," EERL 70-02, July 1970.

58. Trifunac, Mihailo and D.E. Hudson, "Laboratory Evaluations and Instrument Corrections of Strong-Motion Accelerographs," EERL 70-04, August 1970. (N/A)

59. Trifunac, Mihailo D., "Response Envelope Spectrum and Interpretation of Strong Earthquake Ground Motion," EERL 70-06, August 1970.

60. Keightley, W.O., "A Strong-Motion Accelerograph Array with Telephone Line Interconnections," EERL 70-05, September 1970.

61. Trifunac, Mihailo D., "Low Frequency Digitization Errors and a New Method for Zero Baseline Correction of Strong-Motion Accelerograms," EERL 70-07, September 1970.

62. Vijayaraghavan, A., "Free and Forced Oscillations in a Class of Piecewise-Linear Dynamic Systems," DYNL-103, January 1971.

63. Jennings, Paul C., R.B. Matthiesen and J. Brent Hoerner, "Forced Vibrations of a 22-Story Steel Frame Building," EERL 71-01, February 1971. (N/A) (PB 205 161)

64. Jennings, Paul C., "Engineering Features of the San Fernando Earthquake of February 9, 1971," EERL 71-02, June 1971. (PB 202 550)

65. Bielak, Jacobo, "Earthquake Response of Building-Foundation Systems," EERL 71-04, June 1971. (N/A) (PB 205 305)

66. Adu, Randolph Ademola, "Response and Failure of Structures under Stationary Random Excitation," EERL 71-03, June 1971. (N/A) (PB 205 304)

67. Skattum, Knut Sverre, "Dynamic Analysis of Coupled Shear Walls and Sandwich Beams," EERL 71-06, June 1971. (N/A) (PB 205 267)

68. Hoerner, John Brent, "Modal Coupling and Earthquake Response of Tall Buildings," EERL 71-07, June 1971. (N/A) (PB 207 635)

69. Stahl, Karl John, "Dynamic Response of Circular Plates Subjected to Moving Massive Loads," DYNL-104, June 1971. (N/A)

70. Trifunac, M.D., F.E. Udwadia and A.G. Brady, "High Frequency Errors and Instrument Corrections of Strong-Motion Accelerograms," EERL 71-05, 1971. (PB 205 369)

71. Furuike, D.M., "Dynamic Response of Hysteretic Systems with Application to a System Containing Limited Slip," DYNL-105, September 1971. (N/A)

72. Hudson, D.E. (Editor), "Strong-Motion Instrumental Data on the San Fernando Earthquake of February 9, 1971," (Seismological Field Survey, NOAA, C.I.T. Joint Report), September 1971. (PB 204 198)

73. Jennings, Paul C. and Jacobo Bielak, "Dynamics of Building-Soil Interaction," EERL 72-01, April 1972. (PB 209 666)

74. Kim, Byung-Koo, "Piecewise Linear Dynamic Systems with Time Delays," DYNL-106, April 1972.

75. Viano, David Charles, "Wave Propagation in a Symmetrically Layered Elastic Plate," DYNL-107, May 1972.

76. Whitney, Albert W., "On Insurance Settlements Incident to the 1906 San Francisco Fire," DRC 72-01, August 1972. (PB 213 256)

77. Udwadia, F.E., "Investigation of Earthquake and Microtremor Ground Motions," EERL 72-02, September 1972. (PB 212 853)

78. Wood, John H., "Analysis of the Earthquake Response of a Nine-Story Steel Frame Building During the San Fernando Earthquake," EERL 72-04, October 1972. (PB 215 823)

79. Jennings, Paul C., "Rapid Calculation of Selected Fourier Spectrum Ordinates," EERL 72-05, November 1972.

80. "Research Papers Submitted to Fifth World Conference on Earthquake Engineering, Rome, Italy, 25-29 June 1973," EERL 73-02, March 1973. (PB 220 431)

81. Udwadia, F.E. and M.D. Trifunac, "The Fourier Transform, Response Spectra and Their Relationship Through the Statistics of Oscillator Response," EERL 73-01, April 1973. (PB 220 458)

82. Housner, George W., "Earthquake-Resistant Design of High-Rise Buildings," DRC 73-01, July 1973. (N/A)

83. "Earthquakes and Insurance," Earthquake Research Affiliates Conference, 2-3 April, 1973, DRC 73-02, July 1973. (PB 223 033)

84. Wood, John H., "Earthquake-Induced Soil Pressures on Structures," EERL 73-05, August 1973. (N/A)

85. Crouse, Charles B., "Engineering Studies of the San Fernando Earthquake," EERL 73-04, March 1973. (N/A)

86. Irvine, H. Max, "The Veracruz Earthquake of 28 August 1973," EERL 73-06, October 1973.

87. Iemura, H. and P.C. Jennings, "Hysteretic Response of a Nine-Story Reinforced Concrete Building During the San Fernando Earthquake," EERL 73-07, October 1973.

88. Trifunac, M.D. and V. Lee, "Routine Computer Processing of Strong-Motion Accelerograms," EERL 73-03, October 1973. (N/A) (PB 226 047/AS)

89. Moeller, Thomas Lee, "The Dynamics of a Spinning Elastic Disk with Massive Load," DYNL 73-01, October 1973.

90. Blevins, Robert D., "Flow Induced Vibration of Bluff Structures," DYNL 74-01, February 1974.

91. Irvine, H. Max, "Studies in the Statics and Dynamics of Simple Cable Systems," DYNL-108, January 1974.

92. Jephcott, D.K. and D.E. Hudson, "The Performance of Public School Plants During the San Fernando Earthquake," EERL 74-01, September 1974. (PB 240 000/AS)

93. Wong, Hung Leung, "Dynamic Soil-Structure Interaction," EERL 75-01, May 1975. (N/A) (PB 247 233/AS)

94. Foutch, D.A., G.W. Housner, P.C. Jennings, "Dynamic Responses of Six Multistory Buildings During the San Fernando Earthquake," EERL 75-02, October 1975. (PB 248 144/AS)

95. Miller, Richard Keith, "The Steady-State Response of Multidegree-of-Freedom Systems with a Spatially Localized Nonlinearity," EERL 75-03, October 1975. (PB 252 459/AS)

96. Abdel-Ghaffar, Ahmed Mansour, "Dynamic Analyses of Suspension Bridge Structures," EERL 76-01, May 1976. (PB 258 744/AS)

97. Foutch, Douglas A., "A Study of the Vibrational Characteristics of Two Multistory Buildings," EERL 76-03, September 1976. (PB 260 874/AS)

98. "Strong Motion Earthquake Accelerograms Index Volume," Earthquake Engineering Research Laboratory, EERL 76-02, August 1976. (PB 260 929/AS)

99. Spanos, P-T.D., "Linearization Techniques for Non-Linear Dynamical Systems," EERL 76-04, September 1976. (PB 266 083/AS)

100. Edwards, Dean Barton, "Time Domain Analysis of Switching Regulators," DYNL 77-01, March 1977.

101. Abdel-Ghaffar, Ahmed Mansour, "Studies on the Effect of Differential Motions of Two Foundations upon the Response of the Superstructure of a Bridge," EERL 77-02, January 1977. (PB 271 095/AS)

102. Gates, Nathan C., "The Earthquake Response of Deteriorating Systems," EERL 77-03, March 1977. (PB 271 090/AS)

103. Daly, W., W. Judd and R. Meade, "Evaluation of Seismicity at U.S. Reservoirs," USCOLD, Committee on Earthquakes, May 1977. (PB 270 036/AS)

104. Abdel-Ghaffar, A.M. and G.W. Housner, "An Analysis of the Dynamic Characteristics of a Suspension Bridge by Ambient Vibration Measurements," EERL 77-01, January 1977. (PB 275 063/AS)

105. Housner, G.W. and P.C. Jennings, "Earthquake Design Criteria for Structures," EERL 77-06, November 1977. (PB 276 502/AS)

106. Morrison, P., R. Maley, G. Brady, R. Porcella, "Earthquake Recordings on or Near Dams," USCOLD, Committee on Earthquakes, November 1977. (PB 285 867/AS)

107. Abdel-Ghaffar, A.M., "Engineering Data and Analyses of the Whittier, California Earthquake of January 1, 1976," EERL 77-05, November 1977. (PB 283 750/AS)

108. Beck, James L., "Determining Models of Structures from Earthquake Records," EERL 78-01, June 1978. (PB 288 806/AS)

109. Psycharis, Ioannis, "The Salonica (Thessaloniki) Earthquake of June 20, 1978," EERL 78-03, October 1978. (PB 290 120/AS)

110. Abdel-Ghaffar, A.M. and R.F. Scott, "An Investigation of the Dynamic Characteristics of an Earth Dam," EERL 78-02, August 1978. (PB 288 878/AS)

111. Mason, Alfred B., Jr., "Some Observations on the Random Response of Linear and Nonlinear Dynamical Systems," EERL 79-01, January 1979. (PB 290 808/AS)

112. Helmberger, D.V. and P.C. Jennings (Organizers), "Strong Ground Motion: N.S.F. Seminar-Workshop," SL-EERL 79-02, February 1978.

113. Lee, David M., Paul C. Jennings and George W. Housner, "A Selection of Important Strong Motion Earthquake Records," EERL 80-01, January 1980. (PB 80 169196)

114. McVerry, Graeme H., "Frequency Domain Identification of Structural Models from Earthquake Records," EERL 79-02, October 1979.

115. Abdel-Ghaffar, A.M., R.F. Scott and M.J. Craig, "Full-Scale Experimental Investigation of a Modern Earth Dam," EERL 80-02, February 1980.

116. Rutenberg, Avigdor, Paul C. Jennings and George W. Housner, "The Response of Veterans Hospital Building 41 in the San Fernando Earthquake," EERL 80-03, May 1980.

117. Haroun, Medhat Ahmed, "Dynamic Analyses of Liquid Storage Tanks," EERL 80-04, February 1980.

118. Liu, Wing Kam, "Development of Finite Element Procedures for Fluid-Structure Interaction," EERL 80-06, August 1980. (PB 184078)

119. Yoder, Paul Jerome, "A Strain-Space Plasticity Theory and Numerical Implementation," EERL 80-07, August 1980.

120. Krousgrill. Charles Morton, Jr., "A Linearization Technique for the Dynamic Respone of Nonlinear Continua," EERL 80-08, September 1980.

121. Cohen, Martin, "Silent Boundary Methods for Transient Wave Analysis," EERL 80-09, September 1980.

122. Hall, Shawn A., "Vortex-Induced Vibrations of Structures," EERL 81-01, January 1981, PB-

123. Psycharis, Ioannis N., "Dynamic Behavior of Rocking Structures Allowed to Uplift," EERL 81-02, August 1981, PB-

124. Shih, Choon-Foo, "Failure of Liquid Storage Tanks Due to Earthquake Excitation," EERL 81-04, May 1981, PB-

125. Lin, Albert Niu, "Experimental Observations of the Effect of Foundation Embedment on Structural Response," EERL 82-01, May 1982, PB-

126. Botelho, Dirceau L.R., "An Empirical Model for Vortex-Induced Vibrations," EERL 82-02, August 1982, PB-

127. Ortiz, L. Alexander, "Dynamic Centrifuge Testing of Cantilever Retaining Walls," SML 82-02, August 1982, PB-

128. Iwan, W.D., Editor, "Proceedings of the U.S. National Workshop on Strong-Motion Earthquake Instrumentation, April 12-14, 1981, Santa Barbara, California," California Institute of Technology, Pasadena, California, 1981.

129. Rashed, Ahmed, "Dynamic Analysis of Fluid-Structure Systems," EERL 82-03, July 1982, PB-

130. National Academy Press, "Earthquake Engineering Research-1982."

131. National Academy Press, "Earthquake Engineering Research-1982, Overview and Recommendations."

132. Jain, Sudhir Kumar, "Analytical Models for the Dynamics of Buildings," EERL 83-02, May 1983, PB-

Strong-Motion Earthquake Accelerograms
Digitized and Plotted Data

Uncorrected Accelerograms

Volume I

Part	Report No.	NTIS Accession No.
A	EERL 70-20	PB 287 847
B	EERL 70-21	PB 196 823
C	EERL 71-20	PB 204 364
D	EERL 71-21	PB 208 529
E	EERL 71-22	PB 209 749
F	EERL 71-23	PB 210 619
G	EERL 72-20	PB 211 357
H	EERL 72-21	PB 211 781
I	EERL 72-22	PB 213 422
J	EERL 72-23	PB 213 423
K	EERL 72-24	PB 213 424
L	EERL 72-25	PB 215 639
M	EERL 72-26	PB 220 554
N	EERL 72-27	PB 223 023
O	EERL 73-20	PB 222 417
P	EERL 73-21	PB 227 481/AS
Q	EERL 73-22	PB 232 315/AS
R	EERL 73-23	PB 239 585/AS
S	EERL 73-24	PB 241 551/AS
T	EERL 73-25	PB 241 943/AS
U	EERL 73-26	PB 242 262/AS
V	EERL 73-27	PB 243 483/AS
W	EERL 73-28	PB 243 497/AS
X	EERL 73-29	PB 243 594/AS
Y	EERL 73-30	PB 242 947/AS

Strong-Motion Earthquake Accelerograms
Digitized and Plotted Data

Corrected Accelerograms and Integrated
Ground Velocity and Displacement Curves

Volume II

Part	Report No.	NTIS Accession No.
A	EERL 71-50	PB 208 283
B	EERL 72-50	PB 220 161
C	EERL 72-51	PB 220 162
D	EERL 72-52	PB 220 836
E	EERL 73-50	PB 223 024
F	EERL 73-51	PB 224 977/9AS
G	EERL 73-52	PB 229 239/AS
H	EERL 74-50	PB 231 225/AS
I	EERL 74-51	PB 232 316/AS
J,K	EERL 74-52	PB 233 257/AS
L,M	EERL 74-53	PB 237 174/AS
N	EERL 74-54	PB 236 399/AS
O,P	EERL 74-55	PB 239 586/AS
Q,R	EERL 74-56	PB 239 587/AS
S	EERL 74-57	PB 241 552/AS
T	EERL 75-50	PB 242 433/AS
U	EERL 75-51	PB 242 949/AS
V	EERL 75-52	PB 242 948/AS
W,Y	EERL 75-53	PB 243 719

Analyses of Strong-Motion Earthquake Accelerograms
Response Spectra

Volume III

Part	Report No.	NTIS Accession No.
A	EERL 72-80	PB 212 602
B	EERL 73-80	PB 221 256
C	EERL 73-81	PB 223 025
D	EERL 73-82	PB 227 469/AS
E	EERL 73-83	PB 227 470/AS
F	EERL 73-84	PB 227 471/AS
G	EERL 73-85	PB 231 223/AS
H	EERL 74-80	PB 231 319/AS
I	EERL 74-81	PB 232 326/AS
J,K,L	EERL 74-82	PB 236 110/AS
M,N	EERL 74-83	PB 236 400/AS
O,P	EERL 74-84	PB 238 102/AS
Q,R	EERL 74-85	PB 240 688/AS
S	EERL 74-86	PB 241 553/AS
T	EERL 75-80	PB 243 698/AS
U	EERL 75-81	PB 242 950/AS
V	EERL 75-82	PB 242 951/AS
W,Y	EERL 75-83	PB 243 492/AS

Analyses of Strong-Motion Earthquake Accelerograms
Fourier Amplitude Spectra

Volume IV

Part	Report No.	NTIS Accession No.
A	EERL 72-100	PB 212 603
B	EERL 73-100	PB 220 837
C	EERL 73-101	PB 222 514
D	EERL 73-102	PB 222 969/AS
E	EERL 73-103	PB 229 240/AS
F	EERL 73-104	PB 229 241/AS
G	EERL 73-105	PB 231 224/AS
H	EERL 74-100	PB 232 327/AS
I	EERL 74-101	PB 232 328/AS
J,K,L,M	EERL 74-102	PB 236 111/AS
N,O,P	EERL 74-103	PB 238 447/AS
Q,R,S	EERL 74-104	PB 241 554/AS
T,U	EERL 75-100	PB 243 493/AS
V,W,Y	EERL 75-101	PB 243 494/AS
Index Volume	EERL 76-02	PB 260 929/AS